Quaternary Research

doi:10.1017/qua.2020.83

Late Pleistocene and Early Holocene aeolian deposits of Tasmania and their climatic implications

Peter D. McIntosh[a]*, Christina Neudorf[b], Olav B. Lian[c], Adrian J. Slee[a], Brianna Walker[d], Rolan Eberhard[e], Richard Doyle[d], Grant Dixon[e]

[a]Forest Practices Authority, 30 Patrick Street, Hobart, TAS, 7000, Australia
[b]Division of Earth and Ecosystem Sciences, Desert Research Institute, 2215 Raggio Parkway, Reno, NV, 89512, USA
[c]School of Land Use and Environmental Change, University of the Fraser Valley, 33844 King Road, Abbotsford, BC V2S 7M8, Canada
[d]Tasmanian Institute of Agriculture, University of Tasmania, Churchill Avenue, Hobart, TAS 7005, Australia
[e]Department of Primary Industries, Parks, Water and the Environment, 134 Macquarie St., Hobart, TAS, 7000, Australia
*Corresponding author at: Forest Practices Authority, 30 Patrick Street, Hobart, TAS, 7000 Australia E-mail address: peter.mcintosh@fpa.tas.gov.au (P. McIntosh)

(Received January 21, 2020; Accepted August 10, 2020)

Abstract

Late Pleistocene and Early Holocene aeolian deposits in Tasmania are extensive in the present subhumid climate zone but also occur in areas receiving >1000 mm of rain annually. Thermoluminescence, optically stimulated luminescence, and radiocarbon ages indicate that most of the deposits formed during periods of cold climate. Some dunes are remnants of longitudinal desert dunes sourced from now-inundated continental shelves which were previously semi-arid. Others formed near source, often in the form of lunettes east of seasonally-dry lagoons in the previously semi-arid Midlands and southeast of Tasmania, or as accumulations close to floodplains of major rivers, or as sandsheets in exposed areas. Burning of vegetation by the Aboriginal population after 40 ka is likely to have influenced sediment supply. A key site for determining climate variability in southern Tasmania is Maynes Junction which records three periods of aeolian deposition (at ca. 90, 32 and 20 ka), interspersed with periods of hillslope instability. Whether wind speeds were higher than at present during the last glacial period is uncertain, but shells in the Mary Ann Bay sandsheet near Hobart and particle size analysis of the Ainslie dunes in northeast Tasmania suggest stronger winds during the last glacial period than at present.

Keywords: Aeolian; Tasmania; Palaeoclimate; Optically stimulated luminescence (OSL); Thermoluminescence (TL); Thermally-transferred OSL (TT-OSL); Wind speed; Dune; Lunettes; Semi-arid; Last Glacial Maximum (LGM)

INTRODUCTION

Quaternary aeolian deposits (dune sands and thin loess) are found throughout southeast Australia (fig. 4 in Hesse and McTainsh, 2003). Dunes are the most obvious landforms and at present are extensive in the semi-arid zone of the Australian mainland (Bowler and Wasson, 1984; Nanson et al., 1995; Bowler, 1998; Bowler and Price, 1998; Hesse, 2016) and in the subhumid zone of Tasmania (Sigleo and Colhoun, 1982; Dixon, 1996, 1997). Loess is not as extensive in southeast Australia as in New Zealand but is recognised as a regional deposit in the Central Tablelands of New South Wales (Hesse et al., 2003) and along the southern coast, where it is calcareous (Hesse and McTainsh, 2003). Loess has not been mapped in Tasmania, although in the Derwent Valley the term loess was applied to a local deposit of fine sand (Colhoun, 2002) which is more accurately described as a near-source dunesand derived from the adjacent floodplain of the Derwent River.

In marine sediments, dust accumulations are readily recognisable (Hesse, 1994) and it is from the marine record that episodes of dust loss from the land (and their likely correlatives, dune formations on land) can be best defined. The marine records (Hesse, 1994; Hesse and McTainsh, 1999, 2003) show that during the last 400 ka dust accumulation rates were highest during cool periods, particularly in MIS 6 and MIS 2 (as defined by Lisiecki and Raymo [2005]), and generally lower during intervening warmer interglacial and interstadial periods. The broad correlation of aeolian activity and temperature is therefore well-established and

Cite this article: McIntosh, P. D., Neudorf, C., Lian, O. B., Slee, A. J., Walker, B., Eberhard, R., Doyle, R., Dixon, G. 2020. Late Pleistocene and Early Holocene aeolian deposits of Tasmania and their climatic implications. *Quaternary Research* 1–24. https://doi.org/10.1017/qua.2020.83

appears to support the proposition that glacial conditions were not only colder but also drier and possibly windier (Petit et al., 1981; Zhou et al., 1994) than at present, limiting vegetation cover in source areas and favouring erosion. However, Hesse and McTainsh (1999) and Hesse (2016) cautioned against relating increased dune activity to higher wind speeds and argued that lack of stabilising vegetation was the major factor influencing sand movement. While soil dryness will limit vegetation cover, an additional factor to consider is the effect of lower atmospheric CO_2 concentrations favouring grasses over trees during glacial periods (Bragg et al., 2012). Relating aeolian activity and erosional episodes to climate and vegetation change is also complicated by the possible effects of human arrival in Tasmania at about 40 ka (Allen, 1996). The frequency of vegetation burning after Aboriginal arrival is likely to have increased (Fletcher and Thomas, 2010), and the effects of burning may have been exacerbated by the extinction of the herbivorous megafauna at about the same time (Johnson, 2006; Turney et al., 2008; Gillespie et al., 2012; McIntosh et al., 2012; Rule et al., 2012), which is likely to have increased fuel loads, and consequently, fire intensity.

Tasmania is now separated from mainland Australia by the approximately 250-km-wide Bass Strait, but during much of the last glacial period (MIS 2, 3 and 4), i.e., from about 55 to 10 ka, sea level was lower by more than 55 m, exposing a land bridge between Tasmania and Victoria (Blom, 1988; Lambeck and Chappell, 2001). The central Bassian Plain was occupied by a body of water known as Lake Bass during lowest sea levels (–130 m), and Lake Bass Inlet during intermediate sea levels, when it was connected with the ocean to the west. The semi-arid Bassian Plain was a source area for extensive longitudinal dunes, the extremities of which now survive as remnants on land at the Bass Strait margins, notably in northeast Tasmania (Duller and Augustinus, 1997, 2006; McClenaghan, 2006). In coastal regions of western Tasmania (McIntosh et al., 2012), the Bass Strait islands (Eberhard, 2009), and southern Tasmania (Donaldson, 2010; Slee et al., 2012; McIntosh et al., 2012), aeolian deposits of last glacial age also occur, together with Holocene dunes, probably partly derived by reworking of older sands.

In inland Tasmania, three types of aeolian deposits have been recorded: (1) near-source dunes taking the form of clayey or sandy lunettes where they have formed downwind (i.e., east) of lagoons and lakes (Bradbury, 1994; Dixon, 1997) or isolated sandy dunes near floodplains of major rivers (Sigleo and Colhoun, 1982; McIntosh, 2012a); (2) more extensive dunefields where source material has been abundant (Doyle, 1993; Dixon, 1997); and (3) silty or sandy sheet deposits (e.g., McIntosh et al., 2004; Slee et al., 2012), among which one can include minor but significant additions of quartz-rich sand and silt to soils largely formed in parent materials such as doleritic colluvium (Osok and Doyle, 2004).

This paper collates the evidence for the age and mode of formation of Tasmanian aeolian deposits and includes a brief review of the reliability of thermoluminescence (TL), optically stimulated luminescence (OSL), and thermally-transferred optically stimulated luminescence (TT-OSL) dating, which is published in more detailed form in the Supplementary Material. The implications of aeolian activity for deducing climate variation during the last 100 ka are discussed. The review is organised by geographical regions within which present climate is broadly similar. It includes unpublished TL ages for previously undescribed dunes at Rocky Point, King Island, and new TL ages, particle-size analysis and chemical analyses of layers at the Maynes Junction section previously briefly described by McIntosh et al. (2012). The Supplementary Material summarises the methods used for TL and other analyses at these two sites.

Sites described and discussed in this paper are shown in Figure 1. The online Tasmanian Geoconservation Database[1] (TGD) (Comfort and Eberhard, 2011), lists sites of geoscientific interest in Tasmania including deposits of Quaternary age. It includes site locations and scientific information which is publicly available but not formally published, or published only in limited-circulation reports. This database was consulted for 17 sites mentioned or described in this review, and to supplement published information at some sites. Each TGD site is identified by its formal listing code, e.g., TGD site 2249. All radiocarbon ages (except infinite ages) have been calibrated using OxCal version 4.3 (Bronk Ramsey, 2009) and IntCal13 (Reimer et al., 2013) and listed both as reported and calibrated ages with 95% confidence ranges (Table 1).

REVIEW OF TL AND OSL AGES

Many of the ages quoted in this paper were determined by TL methods. Included in the Supplementary Material is a review of the TL, OSL and TT-OSL methods used to date Tasmanian aeolian deposits, and their efficacy. Also included, for context, is a concise history of the development of the early TL dating techniques from which the later luminescence techniques evolved. The notes below summarise the main points of this review.

TL ages derived using multiple aliquot techniques require many aliquots of prepared sample to generate a single age. Therefore, TL dating techniques cannot mitigate the adverse effects of poorly bleached grains that may lead to an age being overestimated. Moreover, the TL signal resets (bleaches) much more slowly that the OSL signal. Thus, TL dating is most applicable to well-bleached deposits (dunes distant from sources and sandsheets will normally fit the well-bleached category) and in these instances they have been shown to yield ages consistent with those found using single aliquot regenerative-dose (SAR) OSL techniques in most cases. Systematic comparisons of ages determined by different methods have not been carried out, but TL ages for dunes at Mary Ann Bay (Slee et al., 2012) determined

[1]http://dpipwe.tas.gov.au/conservation/geoconservation/tasmanian-geoconservation-database

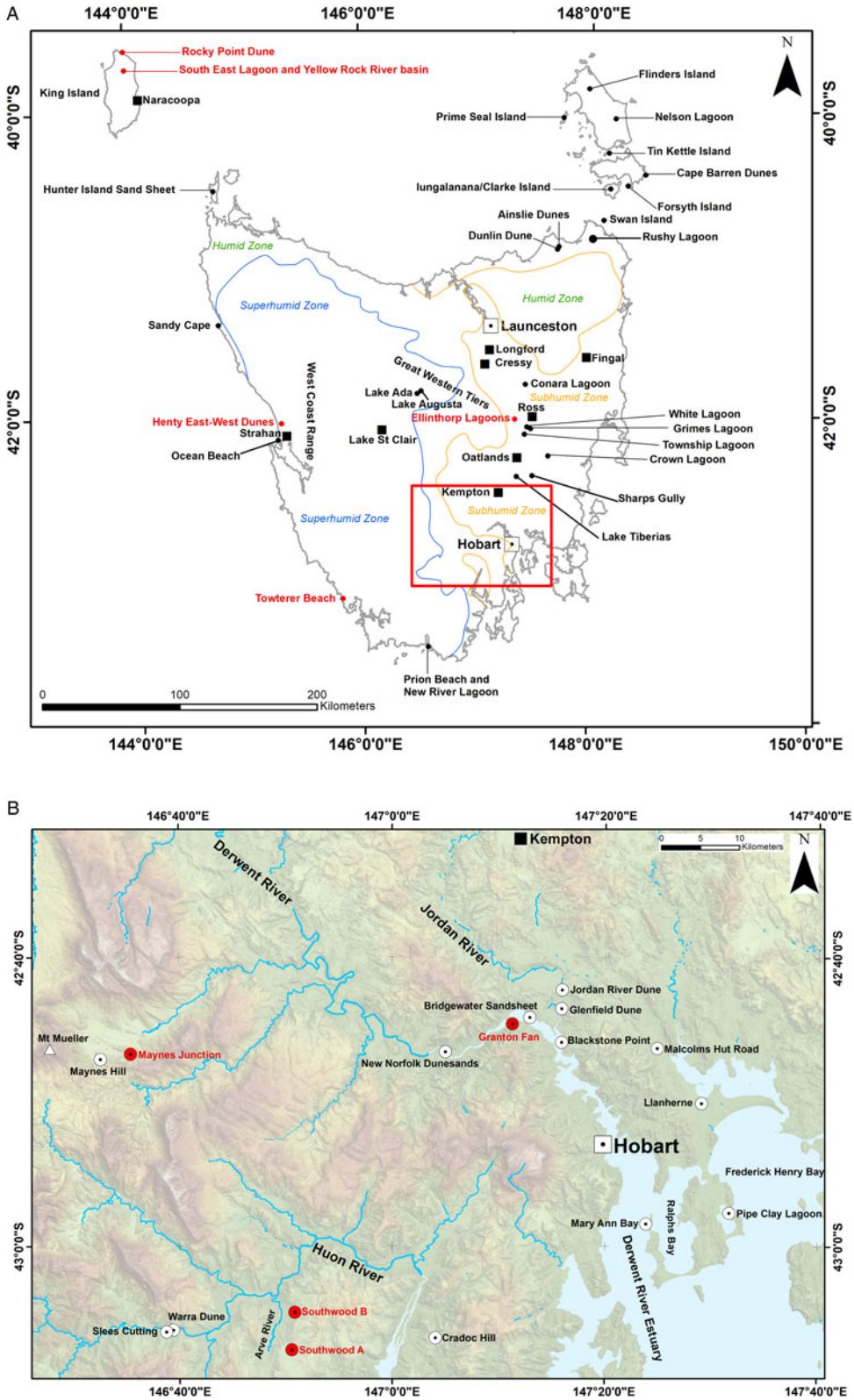

Figure 1. Location of sites discussed in the text. (A) Sites outside the Hobart region and approximate extent of the sub-humid, humid and superhumid zones; (B) sites in the Hobart region. Sites identified by red dots are illustrated with maps or photographs in other figures. Base maps were provided by DPIPWE (Tasmanian Department of Primary Industries, Parks, Water and Environment). (For interpretation of the references to colour in this figure legend, the reader is referred to the web version of this article.)

Table 1. Radiocarbon ages discussed in this paper.

Site	Reference	Material dated	Lab no.[1]	^{14}C age (^{14}C ka BP)[2]	Calibrated age (OxCal) (cal ka BP)[3]
Pipe Clay Lagoon	Colhoun (1977)	organic sediment	SUA151	25.380 ± 0.640	29.57 (28.33–30.90)
			SUA153/2	21.905 ± 0.440	26.24 (25.42–27.24)
Lake Tiberias	Macphail and Jackson (1978)	peat	GaK2239	9.550 ± 0.200	10.80 (10.26–11.35)
Malcolms Hut Road	Sigleo and Colhoun (1982)	charcoal	SUA376	15.740 ± 0.700	19.14 (17.54–20.93)
Blackstone Point		charcoal	SUA306	5.800 ± 0.130	6.61 (6.31–6.90)
		mussels	SUA307	5.600 ± 0.100	6.38 (6.21–6.64)
Bridgewater		charcoal	GaK5593	4.540 ± 0.105	5.18 (4.87–5.47)
Glenfield		charcoal	SUA305	2.055 ± 0.120	2.04 (1.78–2.33)
West Coast Range	Colhoun (1985)	organic sediment	SUA1358	9.050 ± 0.120	10.15 (10.52–9.78)
Rushy Lagoon	Cosgrove (1985)	wood	I-1-11 448A	8.570 ± 0.135	9.59 (9.27–10.13)
Maynes Hill	McIntosh et al. (2008, 2012)	charcoal	Wk17270	24.745 ± 0.288	28.82 (29.47–28.17)
Sharps Gully		charcoal	Wk18972	25.175 ± 0.261	29.29 (28.64–29.93)
Hazards Lagoon	Mackenzie and Moss (2014)	pollen concentrate	OZM134	18.240 ± 0.100	22.11 (21.85–22.37)
Southwood B	Neudorf et al. (2019)	charcoal	Wk20286	>40	not calibrated
Maynes Junction	McIntosh (2012b); McIntosh et al. (2012)	charcoal	Wk26704	26.931 ± 0.351	31.02 (30.50–31.50)
		charcoal	Wk26703	>52.8	not calibrated

[1]SUA, Sydney University Radiocarbon Laboratory (Australia); I, Teledyne Isotopes (USA); Wk, Waikato Radiocarbon Dating Laboratory (New Zealand); OZM, ANTARES AMS Facility, ANSTO (Australia); GaK, Gakushuin University (Japan).
[2]Laboratory values as reported (not rounded).
[3]Median ages, with the 95% probability range in parentheses. Values are rounded to the nearest 10 yr.

by the protocol of Shepherd and Price (1990) were consistent with OSL ages determined by what appears to be a SAR method (Shin, 2013) (Supplementary Material), but unfortunately Shin (2013) provided no experimental detail so a thorough assessment cannot be made.

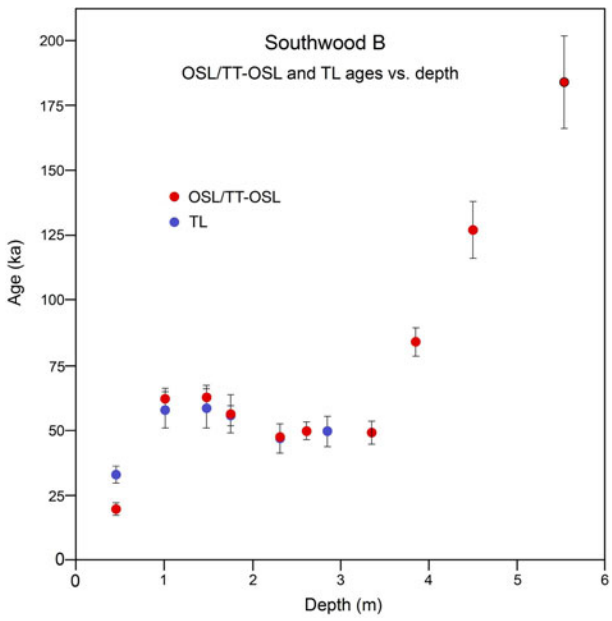

Figure 2. (colour online) Optical ages vs. depth for Southwood B (see Table 3 for data). TL ages were determined using the method of Shepherd and Price (1990) and have been re-calculated using dose rates measured by Neudorf et al. (2019) using neutron activation analysis. The OSL/TT-OSL ages are the weighted mean of the preferred optical ages highlighted in bold in Table 3.

Duller and Augustinus (1997) applied three luminescence dating methods to quartz from the Ainslie dunes. The first two procedures consisted of OSL and TL multiple-aliquot additive-dose total bleach methods applied to the same aliquots. The OSL signal was measured first, followed by the TL signal. A single-aliquot additive-dose OSL procedure was also attempted. The single-aliquot ages were comparable to those found using the multiple-aliquot OSL procedure, and also to three of five TL ages. In light of the SAR protocols developed in the late 1990s (Murray and Wintle, 2000), Duller and Augustinus (2006) re-dated their samples from the Ainslie dunes using this method. An important difference between the SAR protocol and the ones used by Duller and Augustinus (1997) is the ability of the former to correct for sensitivity change, and its inclusion of internal quality control checks. The ages Duller and Augustinus (2006) determined using SAR dating were significantly different from those found using the older multiple-aliquot total bleach methods (Duller and Augustinus, 1997), and are considered to be more accurate. They are consistent with palaeoclimate interpretations for the region. They also cast doubt on the general applicability of the older TL and OSL dating methods.

OSL dating using SAR methods with multi-grain aliquots or single grains has become much more routine in Tasmania (see Supplementary Table S1 in Neudorf et al., 2019), and an extension of the method that uses the TT-OSL signal, which has been shown elsewhere to extend the upper age limit of the method, has been applied at Southwood B (Neudorf et al., 2019). There, a sequence of TT-OSL SAR ages was found to be consistent with the ages previously determined using the TL dating method of Shepherd and Price (1990), but only after the dosimetry used to derive some of the TL ages

Table 2. Stratigraphy and TL ages obtained for coastal dunes at Rocky Point, King Island.

Unit	Depth (m)	TL age (ka)	Description
1.0	0–0.5	–	Light grey (10YR7/1) fine sand; loose
2.0	0.5–1.0	–	Dark grey (10YR4/1) fine sand; firm strength; abundant small roots
3.1	1.0–4.5	**8.32 ± 1.00** (W5021; depth 1.2 m)	Very pale brown (10YR7/4) fine sand; firm strength; no roots
3.2	4.5–5.0	–	Light yellowish brown (10YR6/4) fine sand; firm strength
3.3	5.0–5.9	**6.75 ± 0.65** (W5022; depth 5.6 m)	Brown (10YR 5/3) fine sand; firm strength
4.0	5.9–6.1	–	Strong brown (7.5YR5/6) fine sand; weakly lithified
5.0	6.1–6.4+	**59.9 ± 4.3** (W5023: depth 6.4 m)	Black (7.5YR2.5/1) loamy sand; firm strength

was recalculated based on new radioisotope measurements (Neudorf et al., 2019). Although the apparent consistency between the TL and TT-OSL SAR ages is encouraging (Fig. 2), it should be considered with some caution as the TT-OSL SAR dating technique is still relatively novel. Overall, the evidence summarised above and presented in more detail in the Supplementary Material provides some confidence that the TL ages for the aeolian deposits studied are reasonable, but nevertheless need to be considered with caution. All TL ages quoted in this paper are presented as reported by the University of Wollongong TL laboratory and are identified by their W prefix (e.g., W4237).

COASTAL DUNES AND RELICT LONGITUDINAL DUNES

Bassian Plain

Ainslie dunes

Longitudinal dunes form in line with the direction of the prevailing wind, in areas where the sand supply is low and wind direction is variable (fig. 4 in Wasson and Hyde, 1983). The best developed longitudinal dunes in Tasmania are the Ainslie dunes in the northeast, which are remnants of more extensive dunes originating from source areas in the former Bassian Plain. Duller and Augustinus (2006) dated samples from these dunes by the OSL SAR method which yielded ages in the range 23.8 ± 1.6 to 16.8 ± 0.9 ka, showing that longitudinal dunes at the southern margin of the Bassian Plain were active around the last glacial maximum (LGM), defined as occurring in the period 23.5–17.5 ka in Tasmania (McIntosh et al., 2012). (Previously-obtained OSL ages were as old as 44 ka [Duller and Augustinus, 1997] but were discounted by the later study–see brief review above and the Supplementary Material.) The orientation of the Ainslie dunes is west-northwest to east-southeast (Bowden, 1983; Sharples, 1997), indicating a strong westerly airflow during the LGM and probably a semi-arid or arid climate in the region. The dunes are correctly described as desert dunes. Along the present coast, active dunes are extending in the same east-southeasterly direction.

The maximum thickness of the dunes is not known but most dunes rise 1 to 4 m above the coastal plain. All but one of the 11 samples analyzed by Duller and Augustinus (2006) came from layers less than 2 m deep, so when longitudinal dunes first developed in this area is not known.

South of the Ainslie dunes is an isolated barchan-like dune (Dunlin Dune) in which an exposure (McIntosh et al., 2009, figure 4) shows the present-day podzolised profile overlying a buried podzol profile with similar horizonation. Seven TL ages (McIntosh et al., 2009) show that the dunesand incorporating the lower podzol had accumulated by 21.0 ± 1.5 ka (the age obtained on the sands forming the buried A1 horizon) and the sands which buried this A1 horizon started to accumulate before 15.9 ± 1.3 ka. The significance of the section is that it indicates that there was a wet podzol-forming period in northeast Tasmania during the LGM, after about 22 ka.

Prime Seal Island

Evidence for late Pleistocene aeolian sand movement on the Bassian Plain is supported by a TL age of 56.4 ± 4.3 ka obtained for weakly lithified cross-bedded sands on the northwest coast of Prime Seal Island in the Furneaux Group, Bass Strait (fig. 2 in Eberhard, 2009). During low sea levels this island, which at present reaches a maximum altitude of 165 m above sea level (asl), would have been a low hill lying east of Lake Bass or the later Bass Plain Inlet. At the southern end of Prime Seal Island, a thick sandsheet mantles the western flanks of granite hills and on the present coast is truncated by wave action, forming a sand cliff.

There are no sandy beaches on the west coast of the island, so the likely source of the sandy deposits is the now inundated Bassian Plain. This conclusion is supported by a sequence of TL ages from a 25 m deep section of interbedded aeolian and colluvial sediments exposed in an erosion gully on the southwest coast (Eberhard, 2009). Sands at 21 m depth were dated 37.6 ± 2.3 ka (W4237). Sands at 15 m and 8 m were dated 25.2 ± 2.2 (W4238) and 29.6 ± 2.7 ka (W4239), respectively; within error these ages (mean 27.2 ka BP) are essentially the same. Sands at 1 m depth returned an age of 6.8 ± 0.4 (W4240). The 30–25 ka ages indicate sand deposition at Prime Seal Island at a time approximately coinciding with the period of maximum landscape instability noted on the Tasmanian mainland (McIntosh et al., 2004, 2009, 2012), including the timing of sandsheet deposition at Mary Ann Bay (31–25 ka) and Cradoc Hill (32–25 ka) (see discussion below). An absence of buried soil layers within the Prime Seal Island section indicates potentially continuous sand

Table 3. Southwood B stratigraphy and ages (from Neudorf et al. 2019, table 4).

Measured depth (m)	True depth (m)	TL and radiocarbon sampling depth and age[1] (ka for TL) (cal ka BP for AMS)	OSL/TT-OSL sampling depth and preferred age (ka)[2]	Horizon description[3]	MIS stage[5]
0–0.20	0–0.15			Very dark greyish brown (10YR3/2) loamy sand.	2
0.20–0.40	0.15–0.29			Brown (10YR5/2) loamy sand.	
0.40–0.85	0.29–0.62	W4014 (0.39–0.51 m) As reported: **27.9 ± 2.1** Revised: **32.9 ± 3.1**	W4014 (0.39–0.51 m) **19.7 ± 2.2**	Pale brown (10YR6/3) mottled sandy loam.	2
0.85–1.20	0.62–0.88			Light olive grey (5Y6/2) mottled silty clay.	3
1.20–1.55	0.88–1.13	W4013 (0.96–1.06 m) As reported: **55.4 ± 3.0** Revised **58.0 ± 6.9**	W4013 (0.96–1.08 m) **62.2 ± 4.1**	Light olive grey (5Y6/2) mottled silty loam.	3
1.55–1.95	1.13–1.42			**Weak palaeosol**. Grey (2.5Y6/1) mottled silty clay loam.	3
1.95–2.20	1.42–1.61	W4012 (1.42–1.54 m) As reported: **47.8 ± 3.4** Revised: **58.5 ± 7.6** AMS Wk20286 **>40**	W4012 (1.42–1.54 m) **63.0 ± 4.3**	Light grey (5Y7/1) mottled loam; **charcoal** bands near lower boundary.	3
2.20–2.50	1.61–1.83	W4011 (1.69–1.81 m) As reported: **51.3 ± 3.7** Revised**: 56.4 ± 7.4**	W4011 (1.69–1.81 m) **55.7 ± 4.0**	**Weak palaeosol.** Light grey (5Y7/1) mottled silty loam.	3
2.50–3.00	1.83–2.19			Light olive grey (5Y6/2) mottled medium sand.	3
3.00–4.00+	2.19–3.00	W4010 (2.25–2.37 m) As reported: **52.3 ± 3.5** Revised: **47.0 ± 5.6** W4009 (2.79–2.91 m) As reported: **59.3 ± 3.4** Revised: **49.7 ± 5.9**	SB3 (2.61 m) **49.8 ± 3.5**	Light olive grey (5Y6/2) medium sand; **charcoal**[3] bands at 2.5–2.7 m depth.	3
	3.00–3.65		SB4 (3.35 m) **49.2 ± 4.4**	Grey (2.5Y6/1) sandy loam; bands of coarse sand and brownish yellow (10YR6/8) silty loam.	3
	3.65–4.65		SB5 (3.85 m) **84.1 ± 5.5** SB6 (4.50 m) **127 ± 11**	Grey (2.5Y6/1) loamy sand; scattered **charcoal** fragments.	5
	4.65–4.85			Grey (2.5Y6/1) medium sand with many **charcoal** fragments.	5/6
	4.85–5.95		SB7 (5.53 m) **184 ± 18**	**Weak palaeosol.** Light olive grey (5Y6/2) mottled silty loam (c. 60% sand); **charcoal**[4] band at 5 m depth.	6
	5.95–6.25			Grey (2.5Y6/1) medium sand	6?
	6.25–6.55+			Light olive grey (5Y6/2) silty loam (c. 60% sand)	6?

[1]The radiocarbon age is not calibrated. 'As reported' TL ages, reproduced from McIntosh et al. (2009) were calculated using dose rates measured using thick source alpha counting (U and Th activities) and atomic emission spectroscopy (K activity). 'Revised' TL ages were recalculated using dose rates measured by Neudorf et al. (2019) using neutron activation analysis.
[2]OSL sampling was performed on 7 December 2007; sampling depths are those at centres of sampling tubes. Ages shown are the weighted mean of the preferred OSL and TT-OSL ages for each sample (Neudorf et al., 2019, table 4).
[3]Description according to the Australian Soil and Land Survey Handbook (National Committee on Soils and Terrain, CSIRO, 2019). For a full description see Neudorf et al. (2019).
[4]'Charcoal' in these layers dissolved during the pre-treatment basic wash and could not be dated.
[5]Tentative.

movement and probably desert-like conditions on the eastern margin of the Bassian Plain during the latter part of MIS 3. Minor blow-outs and local renewed accumulation have also occurred on Prime Seal Island in the mid-Holocene (7–4 ka; Eberhard, 2009).

Flinders Island and the Furneaux group

Flinders Island, the largest of the Furneaux Group of islands in northeast Tasmania, is extensively mantled by aeolian sands including well-developed dunes orientated east-west, which Kershaw and Sutherland (1972) described as parabolic. These dunes extend several kilometres inland. Most of these deposits are now stable and vegetated, and where the sand is calcareous, lithified as calcarenite rock. Sutherland and Kershaw (1971) mapped five dune types. One type (Trousers Point aeolianite) is only found locally on the west coast of the island, and may be a variant of one of the other more extensive dune types which were named (1) Palana limestone dunes; (2) inland siliceous dunes (parabolic); (3) unconsolidated parabolic dunes; and (4) beach ridge and frontal dunes. The Palana limestone dunes are in places overlain by the other dune types and are undoubtedly the oldest, and their occurrence as sea stacks indicate that they once extended over the Bassian Plain during low sea levels. Kershaw and Sutherland (1972) suggested they were at least as old as the last interglacial (MIS 5) and probably older, given their likely cold-climate origin. The siliceous east-west parabolic dunes (Types 2 and 3) are likely to have formed at the same time as the similarly siliceous longitudinal Ainslie dunes on the Tasmania mainland, i.e., during MIS 2 and possibly earlier. The beach ridge and frontal dunes relate to the recent coastline and formed in the Holocene. However, within all mapped deposits, the predominant formation may contain remnants of earlier deposits. No deposits have been systematically dated.

The origin of undated longitudinal dunes elsewhere in the Furneaux Group islands (Forsyth Island, Tin Kettle Island, and Swan Island), and on the eastern side of Cape Barren Island (TGD sites 3008, 3011, 2310 and 2307) is more problematic. At all four sites the dunes run inland from sandy beaches to their west, so a Holocene origin cannot be ruled out, but the east-west orientation of the dunes matches the orientation of dunes on Flinders Island and one could infer that some of these deposits are also remnants of longitudinal desert dunes. On lungtalanana (Clarke Island), inland longitudinal dunes were interpreted to have a similar age to the Ainslie dunes (Bradbury, 2014).

Hunter Island

Dune fields on Hunter Island in northwest Tasmania (TGD site 2451) resemble longitudinal dunes in places but are undated. In the TGD record, brown sands are considered to be of Holocene age but strongly bleached (podzolised) sands are assigned a last interglacial age. However, podzolisation can occur in sands as young as 7 ka, notably at Towterer Beach (TGD site 2894, considered below), so the suggested last interglacial origin for podzolised sands on Hunter Island cannot be justified. More plausibly, these are glacial age sediments deposited during MIS 2–4 (Eberhard, 2017).

King Island

King Island, at the western entry to Bass Strait, has a similar relict aeolian terrain to that of Flinders Island to the east. On King Island, aeolian landforms can be broadly differentiated into lithified calcareous inland dunes, and more recent sandsheets and beach-backing dunes on the coastal fringe. These are interpreted to have formed in the last interglacial period ('old dunes') and Holocene ('new dunes') respectively, as described by Jennings (1957, 1959).

New TL ages have been obtained for the beach-backing 'new dunes' (Jennings, 1957) at Rocky Point on the northeast coast of King Island (Fig. 3; see Supplementary Material for TL methods and derivation of TL ages). The site is a sandblow within an otherwise vegetated coastal dune complex. The deflated upper portion of the dune is formed in fine, loosely compacted sand with a buried soil horizon at a depth of 0.5 m, below which are further discontinuities, interpreted to be palaeosols, at 1, 5.9, and 6.1 m depths (Fig. 3). On the basis of these discontinuities, five stratigraphic units have been distinguished (Table 2). At the base of the sandblow is a strong brown, weakly lithified sand (Unit 4) covering black loamy sand (Unit 5). The basal loamy sand (Unit 5) was dated 59.9 ± 4.3 ka (W5023) and the overlying non-lithified sand above (Unit 3) returned TL ages of 8.32 ± 1.00 ka (W5021) and 6.75 ± 0.65 ka (W5022) (Table 2). The two younger ages are out of stratigraphic order but their errors overlap. The uppermost sample W5021 exhibited a short temperature plateau suggestive of incomplete re-setting of the TL signal.

These results indicate that the Rocky Point dune is formed chiefly in Holocene sand, consistent with foredune development by deflation of sand pushed ashore by wave action during the most recent marine transgression. However, the base of the dune is evidently a relict deposit including a buried soil horizon, formed under a glacial climate towards the end of MIS 4. We conclude that it is misleading to assume that the present-day sandy coastal landforms on King Island, and indeed elsewhere on the Tasmanian coast, are solely the product of Holocene processes. We also note that the TL result of 59.9 ± 4.3 ka (W5023) for the deepest Rocky Point deposit bears comparison with a result of 55.6 ± 3.0 ka from dunesands at Sandy Cape, 200 km to the south (McIntosh et al., 2012), and 56.4 ± 4.3 ka from dunesands at Prime Seal Island 300 km to the east (discussed above). These data emphasise the broad extent of aeolian activity during late MIS 4/early MIS 3.

At inland sites on King Island, the lithified calcareous 'old dunes' were assumed to be significantly older than the dunes that fringe the coastline (Jennings, 1957, 1959; Murray-Wallace and Goede, 1995; Calver, 2007), although none of these dunes were dated or described in detail. Jennings

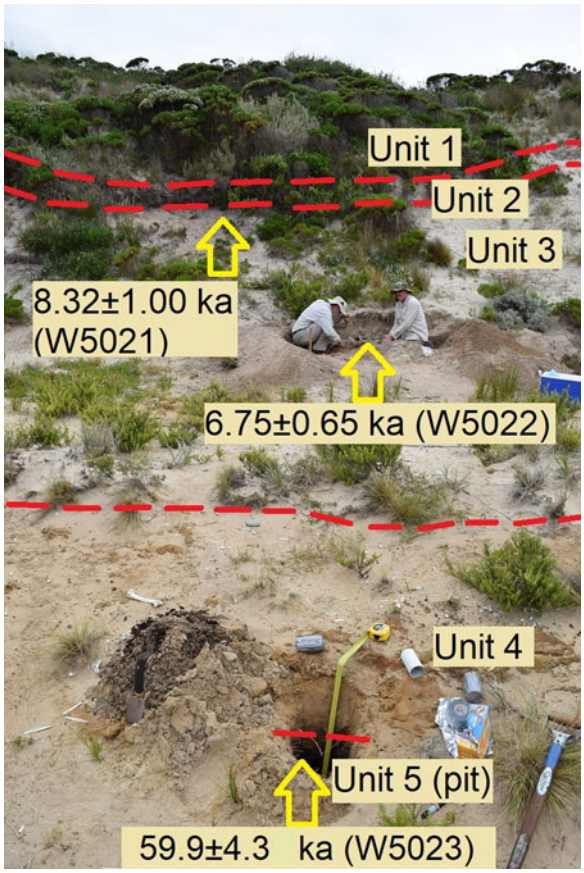

Figure 3. (colour online) Dated dunesands within a sandblow at Rocky Point, King Island. The bulk of the dune (Units 1–3) is formed in loosely compacted sand of Holocene age. The base of the sandblow rests on darker, more coherent sand (Unit 4), which mantles older black loamy sand (Unit 5).

(1957, 1959) speculated that these old dunes were formed during the last interglacial and were subsequently uplifted to their current height of 20 m asl. However, this view was disputed by Murray-Wallace and Goede (1995) who suggested, on the basis of ESR and amino-acid racemisation ages of shells in inland lagoons, that the dunes were substantially older than MIS 5e. An interglacial origin for the calcareous inland dunes is considered unlikely because source material in the form of calcareous marine sediments is likely to have been in short supply during high sea levels, but plentiful during low sea levels when the Bassian Plain was exposed.

Jennings (1957), in his survey of the landscape in the vicinity of the now drained South East Lagoon in the Yellow Rock River catchment, recognised an ancient shoreline and inland lithified 'old' dunes at the catchment's eastern margin, 11 km east of the present west coast of the island. Later field observations by the authors of this article combined with air-photograph interpretation, has allowed the dunes to be mapped in more detail (Fig. 4). The dunes are composed of a thin 1 m-thick veneer of white loose sand overlying yellow/brown strongly lithified sand. Surface layers contain small angular bedrock fragments, likely to be Aboriginal artefacts produced by hunting parties that camped on the dunes adjacent not only to the original marine inlet to the west but also adjacent to lakes and swamps to the immediate east, dammed by barchan and longitudinal dunes (Fig. 4).

Observations suggest that the arcuate dune ridges on the eastern margin of the Yellow Rock River basin formed behind a beach, on the flanks of older dunes and lagoons to the east. The dune ridges probably formed in an interglacial period pre-dating the last interglacial (Murray-Wallace and Goede, 1995) when the Yellow Rock River basin was a large tidal estuary connected to Bass Strait. The basin is bounded at the 20 m asl contour by low benches and dunes, which are interpreted to mark the margin of a large marine bay that once filled the basin. The inferred marine bench at 20 m asl fits well with the estimated uplift rates for King Island and north-western Tasmania since the mid-Quaternary (MIS 9) (Mazengarb and Stevenson, 2016), indicating that the Yellow Rock River basin was a bay during MIS 9. The 20 m contour also corresponds with the base of raised coastal sea cliffs located south of Naracoopa in southeastern King Island (Jennings, 1959; TGD site 2619) and with the base of the old sea cliff in the Corinna-Pieman area of the north-west Tasmanian mainland (Twidale, 1957). We infer that as the land rose the estuary slowly drained to form South East Lagoon, the last remnant of which was destroyed by agricultural activities in the late 20th century. Further evidence for a marine origin for this embayment is the offshore bar mapped by Jennings (1957) immediately west of South East Lagoon, no longer evident in recent imagery. In all likelihood this landform has been significantly disturbed by the same agricultural practices that drained the lagoon. The Yellow Rock River basin has been further isolated from the sea by dune ridges of probable last glacial and Holocene-age at the mouth of the basin (Fig. 4).

It is notable that the 20 m contour on the eastern side of King Island almost meets the 20 m contour on the western side (Fig. 4), indicating that King Island may originally have been two islands; the dunes east of the Yellow Rock River basin may originally have formed part of a spit which eventually closed the shallow marine channel separating the islands.

Tasmanian West Coast

On the west coast of Tasmania near Sandy Cape, dunes have been TL dated in the range 56–21 ka (McIntosh et al., 2012) as well as to the Holocene (13–9 ka). The older dunes have lost their original morphology as they have been partly eroded and overwhelmed by later sand movement. It is likely that the older deposits at Sandy Cape, like the Ainslie dunes and those on Prime Seal Island, are the remains of a longitudinal linear dune field that once extended across the continental shelf, which was much wider during the last glacial period (Lambeck and Chappell, 2001); the dunes' ultimate origin may have been the coast several kilometres to the west. In contrast, beach-backing dunes to the south at Ocean Beach near Strahan are of Late Holocene age (Sharples et al., 2020).

Although it has been suggested (Sharples, 1996, p. 63) that the active Henty dunes north of Strahan (Fig. 5), which reach

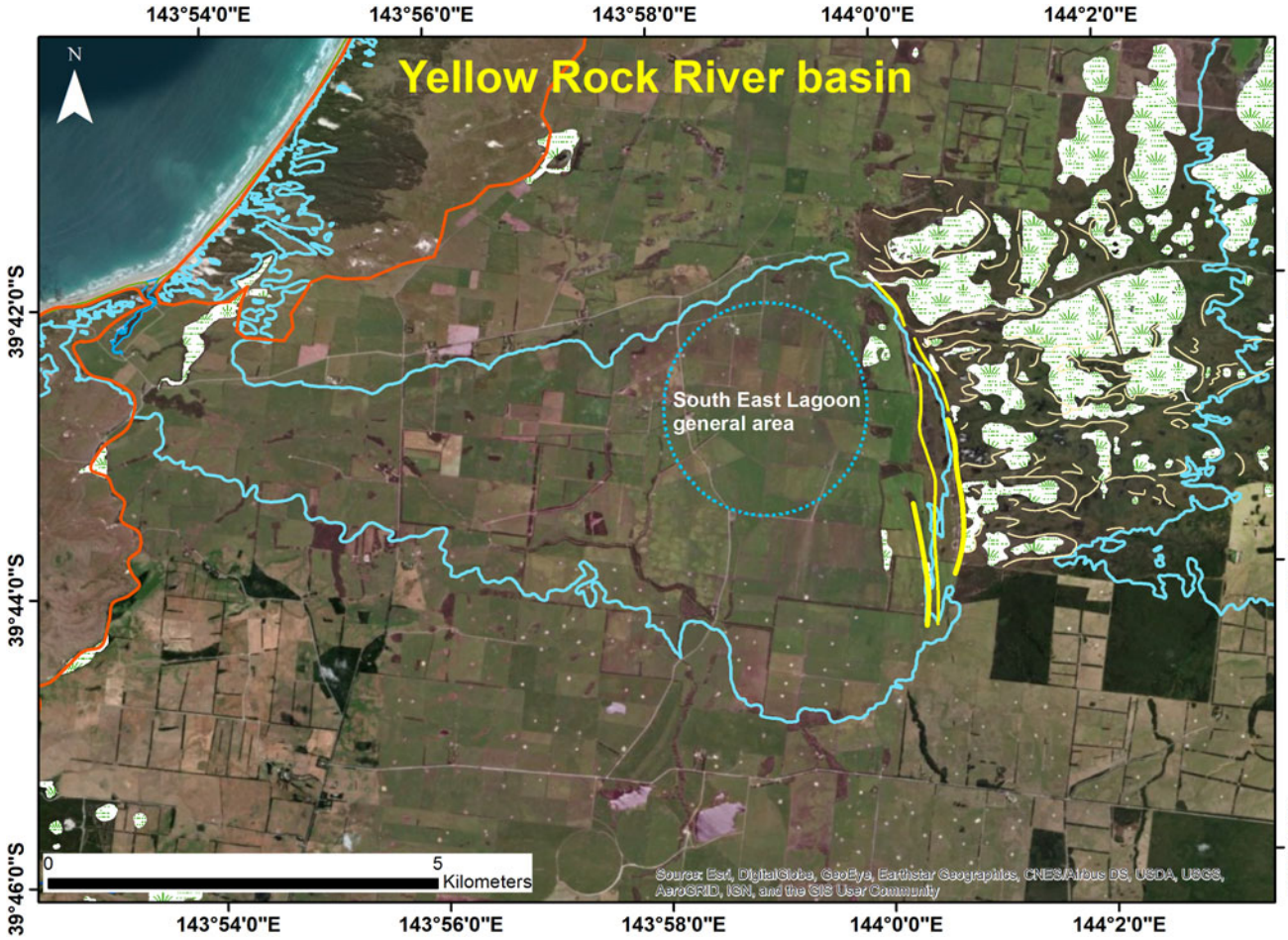

Figure 4. In the centre of the image the Yellow Rock River basin is outlined by the 20 m contour and low cliffs (blue line). Red-brown lines indicate the extent of the Holocene-age coastal dunes. The yellow lines at the eastern side of the basin mark three arcuate beach-backing dunes. White areas with reed symbols east of the arcuate dunes indicate lakes and swamps. Intervening thin yellow lines indicate dunes trapping the lakes and swamps. On the right of the image the 20 m contour shown in blue shows the likely extent of an earlier marine incursion from the east, which may have extended into the Yellow Rock River basin prior to dune development, dividing the island in two. (For interpretation of the references to colour in this figure legend, the reader is referred to the web version of this article.)

thicknesses of 145 m, may have both Holocene and Pleistocene components, the dunes do not have the longitudinal morphology characteristic of desert dunes and evidence of a last glacial age is lacking. It is likely that the active Henty dunes (outlined in red in Figure 5) are entirely of Holocene age, supplied by sand from the extensive sandy beaches north of Strahan. However, within the area of active dunes, dunes with more complex morphology are evident (Fig. 5) and these are likely to be remnants of older dunes.

Inland from the active Henty dunes are stable vegetated dunes. A prominent set of dunes having slip faces orientated approximately east-west (Fig. 5; TGD site 3234; McIntosh 2012b) are interpreted to be transverse dunes resulting from the effect of unimodal winds on a plentiful sand supply (Reffet et al., 2010). Their morphology indicates a source from the Henty River floodplain (to the north) rather than the coast (to the west). Formation by northerly or north-northwesterly winds rather than westerlies (that prevail at present) is inferred. A TL age of 10.1 ± 1.2 ka was obtained from a sample taken at 1.5 m depth on the fourth crest counting from the south (McIntosh, 2012b; Fig. 4), probably indicating increased supply of sediment to the Henty River floodplain at around this time, enhanced by the rapid melting of glaciers in the West Coast Range, which was complete by 9.050 ± 0.120 ^{14}C ka BP (10.52–9.78 cal ka BP) (Colhoun, 1985; Table 1).

Four periods of dune formation can be deduced from the aeolian landforms (Fig. 5): the modern Henty Dunes which are presently active and periodically advancing; historic dunes which buried the railway after 1960; the transverse dunes with east-west orientation of early Holocene age; and older dunes of unknown age, with complex morphology that has probably been highly influenced by a combination of local induration and deflation.

Southwest Tasmania

Longitudinal dunes in southwest Tasmania are well developed at Towterer Beach (TGD site 2894; Baynes, 1990; Fig. 6) where TL ages of 7.1 ± 2.3 and 5.2 ± 1.7 ka (W2093 and W2095) were obtained from podzolised sediments.

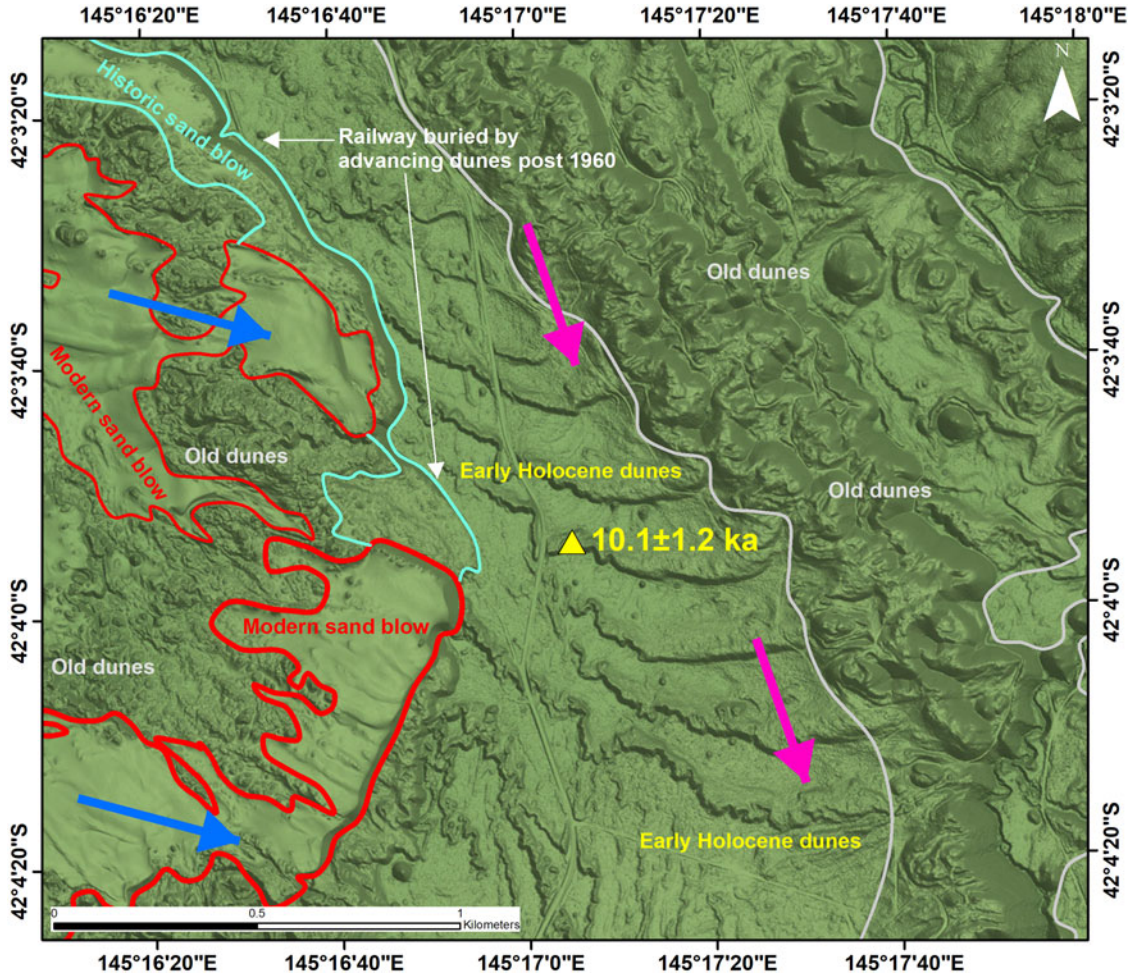

Figure 5. The Henty east-west transverse dunes (TGD site 3234) illustrated in the centre of this figure have been TL dated 10.1 ± 1.2 ka (McIntosh, 2012b) at the location shown by the yellow triangle. The orientation of the dunes indicates accumulation from a northerly direction (pink arrows). In contrast dunes which are active at present (the Henty Dunes, shown in red and light blue outline) are sourced from the west-northwest (dark blue arrows). (For interpretation of the references to colour in this figure legend, the reader is referred to the web version of this article.)

These ages, the dunes' local extent, and the local beach sand supply, together indicate that the dunes formed at the end of the mid-Holocene sea level high-stand around 7.5 ka (Lewis et al., 2013) and that they are not remnants of a glacial-age dunefield. Likewise, most beach-backing dunes and sandsheets extending inland from most major beaches on the southwest coast appear to be of Holocene age. However, some of these features may incorporate relict sands which predate the most recent marine transgression (Eberhard et al., 2015).

Dunes on the Prion Beach sandspit and on the coast east of the adjacent New River Lagoon have been described and OSL dated by Cullen and Dell (2013), who identified at least three stages of Mid- to Late Holocene dune development on the Prion Beach spit, spanning ages between 2.2 ± 0.5 to 6.2 ± 2.8 ka. Older OSL ages of 116.8 ± 34.8 and 126.2 ± 33.8 ka in sands in forested terrain east of New River Lagoon were interpreted by Cullen and Dell (2013) to date remains of dunes associated with a last interglacial spit. However, these older ages have large errors which do not allow confident assignment to climate stages. One dune on Prion Beach (PB12), which is situated on the northeast side of New River Lagoon (i.e., isolated from the dunes forming the Holocene spit), was OSL dated 24.8 ± 7.0 ka (fig. 2 in Cullen and Dell, 2013) showing that some sands were accumulating during the last glacial period. These can be classified as near-source dunes, derived either by deflation by westerly winds of alluvial sands from the now flooded New River floodplain, or by reworking of older dunes.

Inland sandsheets, lunettes and isolated dunes

Midlands sandsheets

A complex distribution of aeolian sandsheets occurs in the Macquarie River catchment in the Tasmanian Midlands between Ross and Cressy (Dixon, 1997; TGD site 2249), where sand has been deflated from floodplains of the Macquarie River and its tributaries such as the Isis River onto the windward slopes of hills in several areas (e.g., onto Mt.

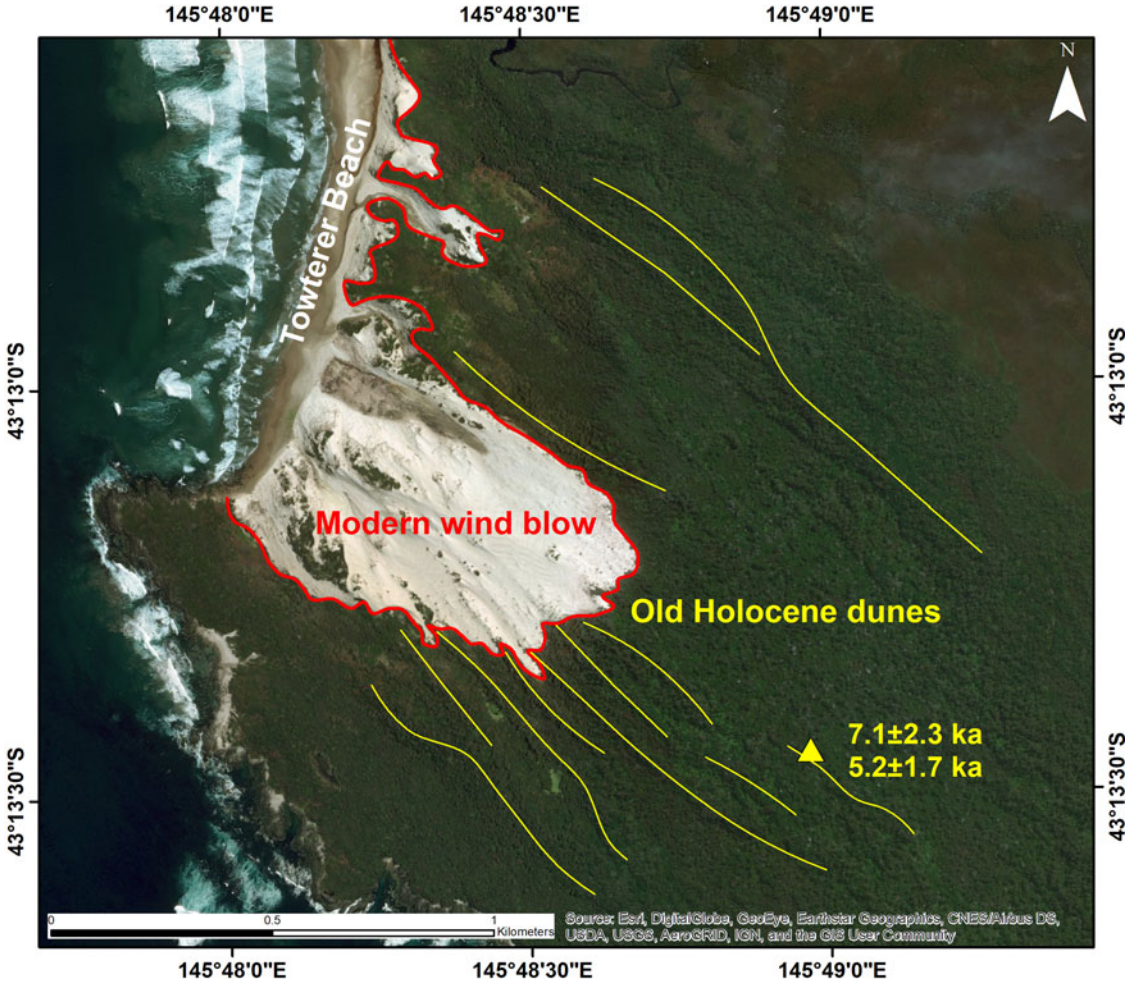

Figure 6. The Holocene TL ages obtained for vegetated dunesands (indicated by yellow lines) inland from Towterer Beach, southwest Tasmania, indicate that these sands are not remnants of longitudinal dunes developed when the sea level was low. (For interpretation of the references to colour in this figure legend, the reader is referred to the web version of this article.)

Augusta) (Matthews, 1975, 1983; Pinkard, 1980). Similar sandsheets also occur in the Fingal Valley, and around Longford where they are mapped as Panshangar soils (Doyle, 1993), and as far south as Kempton (McIntosh, 2015a). Individual sandsheets cover less than a hectare to more than 10 km^2. Minor sand movement continues to the present in the form of sporadic blowouts and areas of recently remobilised sand. However, the overall stability of the sands and river floodplains at present suggests that the sandsheets are cold-climate deposits and formed when sand supply was greater and/or vegetation cover was limited by aridity. None of the sandsheets have been dated.

Lunettes

Lunettes downwind (east of) seasonal lakes are common in the Midlands of Tasmania. Several lagoons and associated lunettes have been listed in the TGD: Lake Tiberias, Conara Lagoon, Nelson Lagoon, Grimes Lagoon, Township Lagoon and White Lagoon (TGD sites 2632, 2248, 2270, 2627, 2629 and 2634, respectively) and a group of small features (Ellinthorp Plains Lunette Systems; TGD site 2630; Fig. 7). Lunettes are also found in the dry lowlands of southeast Tasmania, at Pipe Clay Lagoon (now flooded by the sea) and the adjacent Rushy Lagoon (Colhoun, 1977); and in northeast Tasmania at Rushy Lagoon and the adjacent Mygunyah Lagoon (Cosgrove, 1985). However, many lagoons and associated lunettes remain unlisted.

The Ellinthorp lunettes (Fig. 7) clearly formed during westerly winds. In the present subhumid climate they are vegetated and stable. The concentration of lagoons and lunettes at this location may result from their position at the foot of the uplands (Great Western Tiers) which reach altitudes of >1100 m asl to the west, where seasonal snowmelt is likely to have enhanced sediment supply to the previously semi-arid lowlands.

The lagoon and associated lunette at Lake Tiberias (Macphail and Jackson, 1978; Dixon, 1997) covers about 10 km^2 of a 21 km^2 catchment and is the largest lagoon and associated lunette in Tasmania. The nearest weather station at Oatlands has a mean annual rainfall of 547 mm (Bureau of Meteorology [BOM], 2020, record for station 93014). The

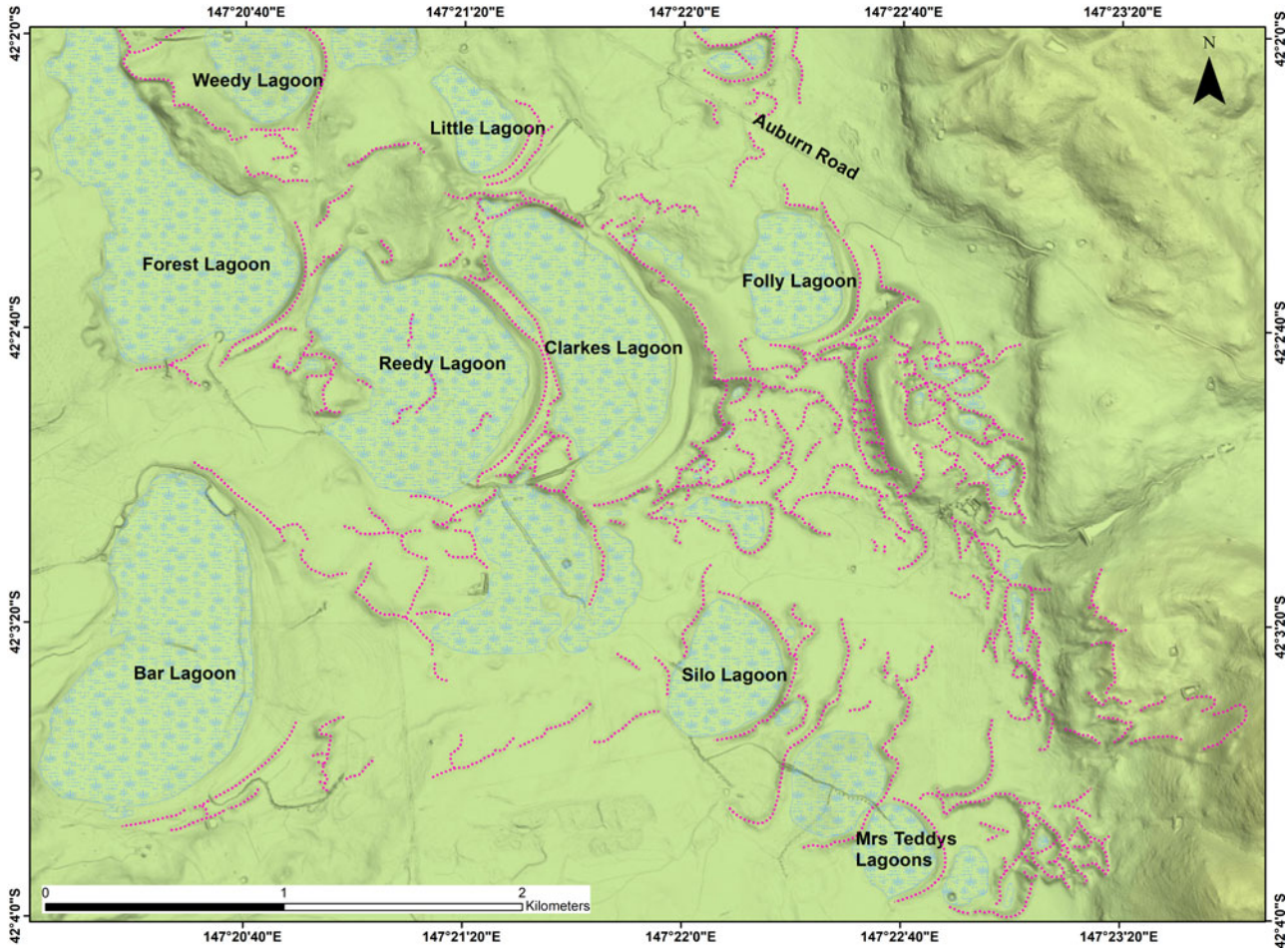

Figure 7. The Ellinthorp Plains Lunette Systems (TGD site 2630) in the Tasmanian Midlands. Pink dotted lines follow dune crests. (For interpretation of the references to colour in this figure legend, the reader is referred to the web version of this article.)

lunette is about 4 km long. Lake Tiberias is the only lagoon in the Tasmanian Midlands to have been investigated palynologically: Macphail and Jackson (1978) cored the lake sediments and obtained "215 cm of well humified sedge peats overlying an unknown depth of lacustrine clays."

The clays were sampled to 283 cm depth. Clays below 251 cm depth contained very little pollen. Layers at 251–210 cm depth were dominated by *Eucalyptus* and *Phyllocladus* pollen deduced to be derived from forests on higher humid uplands to the west (the Great Western Tiers). *Eucalyptus* and *Pomaderris* pollen from the same presumed source dominated in layers from 210 cm to the surface. Although Macphail and Jackson (1978, figure 3) attributed the presence of significant amounts of chenopod pollen between 251–210 cm depth to long-distance transport, possibly from the mainland, the fact that the chenopod pollen percentage declined to very low values above 210 cm, despite chenopod communities still being present on the mainland, and that lunette morphology indicates a prevailing wind from the west-northwest rather than from the north, suggests that the alternative interpretation considered by Macphail and Jackson (1978, p. 293) that the pollen record reflects a chenopod "cold steppe community in the Midlands, analogous to the Gramineae-Chenopod associations of (hot) semi-arid to arid regions of mainland Australia" is more likely to be correct.

Above 135 cm depth, grasslands and sedges dominated the local pollen assemblage. *Myriophyllum* pollen at 251–135 cm depth indicated at least seasonally wet conditions. A ^{14}C age of 9.550 ± 0.200 ^{14}C ka BP (10.26–11.35 cal ka BP) (Table 1) was obtained on the base of the peat in a second core. As peats can be contaminated by percolating humic acids (as probably occurred in peats at Pipe Clay Lagoon in southeast Tasmania [Colhoun, 1977]) this age is probably a minimum for the beginning of peat accumulation at this site.

In summary, it can be deduced that the clays below 251 cm, containing very little pollen, were probably deposited quickly, perhaps by floods following rapid snow melt in the uplands to the west during the last glacial period. If the chenopod pollen is indeed derived from local sources, it can be deduced that a more stable landscape dominated by chenopods and low shrubs followed, as reflected in the *Myriophyllum*/chenopod pollen record, indicating the presence of a seasonal shallow lake surrounded by a semi-arid or arid herb/shrubland. Onset of Holocene subhumid conditions (recorded in peat above 210 cm depth) led to expansion of eucalypts and grasslands in the surrounding land. Throughout the record *Eucalyptus*

pollen (and for a time, *Phyllocladus* pollen) rained onto the lake from distant western (and wetter) upland sources.

Most lunettes are developed in quartzo-felspathic aeolian sediments, and, like their mainland counterparts, are clayey if derived from the dry lake bed or sandy if derived from beaches formed during high lake levels (Bowler and Wasson, 1984). Exceptions are lunettes derived from clayey weathered doleritic sediments in the subalpine environment of the Central Plateau, notably those at lakes Ada and Augusta at 1100 m asl (TGD sites 2703 and 3144; Bradbury, 1994).

Lunette sediments provide unique opportunities for deducing climate variation, as their sediment types and rates of accumulation are sensitive to water levels in their associated lakes. Unfortunately, no lunette sediments in Tasmania have been systematically dated, although Lourandos (1970), quoted by Sigleo and Colhoun (1982), obtained Holocene ages for Aboriginal hearths in the upper part of the sandy lunette at Crown Lagoon, 22 km east of Oatlands. On the basis of wood dated 8.570 ± 0.135 ^{14}C ka BP (9.27–10.13 cal ka BP) (Table 1) Cosgrove (1985) deduced that the most recent accumulation of sand on the lunette at Rushy Lagoon occurred in the early Holocene.

At White Lagoon, Sigleo and Colhoun (1982) described a basal sandy clay unit overlain by about 30 cm of sand in turn overlain by a younger clay unit. The sequence implies two periods of relative dryness (represented by the clays eroded from the dry lake bed) separated by a period in which White Lagoon was full and sand dunes, derived from remobilised beach sand, accumulated. Sigleo and Colhoun speculated, on the basis of 'rubification' of the palaeosol developed in the lower clayey unit, that it accumulated during the last interglacial period, but the layer may well be younger. Dating of the White Lagoon lunette section and palynological examination of the lagoon sediments would provide useful information for elucidating the climate history of the Tasmanian Midlands.

Sandsheets and dunes of southern Tasmania

Lower Derwent estuary

East of the lower Derwent estuary, and notably on South Arm Peninsula and Seven Mile Spit around Frederick Henry Bay, extensive sandsheets and dunes are present.

At Llanherne on Seven Mile Spit, Donaldson (2010), reported by McIntosh et al. (2012, site 23), obtained TL ages of 53.8 ± 3.5 and 26.1 ± 3.5 ka for cross-bedded sands. The older sands accumulated during MIS 3 when sea levels were oscillating at about 50 m below their present level and the younger sands accumulated during MIS 2 when sea levels were ca. 100 m below their present level. The dunes at Llanherne accumulated near the northern limit of a thick sandsheet that draped the wide southern extent of the Coal River valley and probably extended southwards over the area east of the Derwent River that is now partly submerged under Frederick Henry Bay. At Llanherne the sands overlie sandy clays that may have formed in the last interglacial.

The most likely source of these extensive sandsheets and dunesands is the (now flooded) Derwent River floodplain, about 20 km southwest of Llanherne. Deflation and deposition during southerly or southwesterly winds is likely. As no palaeosol is present between the sands dated 53.8 and 26.1 ka at Llanherne, the sands may have accumulated steadily as the Derwent River fan prograded southwards following the fall of sea level to its minimum of about –130 m. The ultimate source of the extensive aeolian deposits of the lower Derwent estuary and east of it is likely to be glacial outwash from the Lake St. Clair region of the upper Derwent River catchment. During the last glacial period the lower reaches of the Derwent River were probably braided and would have carried large volumes of gravel, silt and sand during spring flows. Some sediment was also undoubtedly sourced locally from the lower Derwent valley where massive erosion has periodically occurred in the steep side valleys cut into Permo-Triassic sedimentary rocks, producing alluvial fans many metres thick (Wasson, 1977; Fig. 8).

We surmise that when sea levels rose in the Holocene, many lagoons and lunettes near the coast and their associated uncemented and incompetent sandsheets were eroded, forming the relatively shallow inlets of Frederick Henry Bay and Ralphs Bay. As a result, only the higher remnants of the last glacial aeolian landscape are now preserved, mostly where the sandsheets are underlain by erosion–resistant hard rock formations. Such sandsheet remnants are preserved on the South Arm Peninsula, which has a sand cover which survived rising sea levels because of its underlying dolerite and Permo-Triassic sedimentary rocks. At Pipe Clay Lagoon, Colhoun (1977) identified last interglacial marine sands at 3–4 m above present sea level and overlying these were freshwater organic-rich sands radiocarbon dated 25.380 ± 0.640 ^{14}C ka BP (28.33–30.90 cal ka BP) to 21.905 ± 0.440 ^{14}C ka BP (25.42–27.24 cal ka BP) (Table 1). These sands were in turn overlain by aeolian sands of presumed LGM age. Aeolian activity may have begun earlier than 25 ka, as contamination of the dated organic layers with humic acids was recognised to be a problem.

Nearby, at Mary Ann Bay, 7.5 m of calcareous aeolian sands up to 24 m asl overlie a thin sequence of sands and palaeosols, which in turn overlie weathered dolerite (Slee et al., 2012; Shin, 2013). The sands were assigned a last interglacial age and marine origin on the basis of electron spin resonance dating of shells in their upper layers (Murray-Wallace and Goede, 1991; Murray-Wallace and Woodroffe, 2014, p. 218). (McIntosh et al. [2012] updated the species list provided by Colhoun et al. [1982], who noted shells of 48 species, ranging from large weathered and damaged *Pecten* and *Ostrea* shells to the micro-gastropod *Microdiscula*.) However, two TL and two OSL ages obtained by Slee et al. (2012) and Shin (2013), respectively, overlooked by Murray-Wallace and Woodroffe (2014), demonstrate that the sands were deposited around 31–25 ka when sea levels were about 90–100 m below present sea level (Lambeck and Chappell, 2001; Compton, 2011) and falling rapidly. This age range for the sands rules out a marine origin, and together

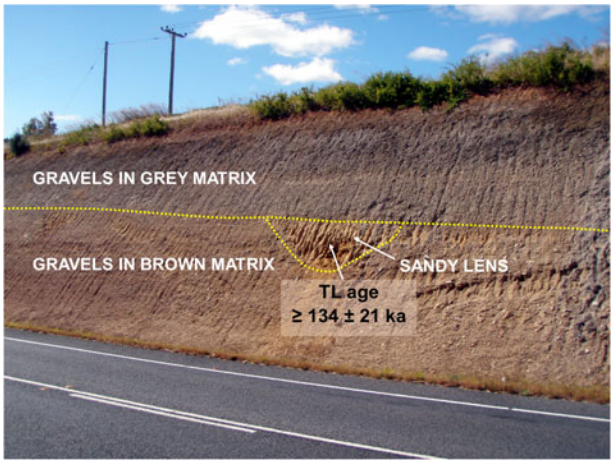

Figure 8. (colour online) The alluvial fan at Granton, approximately 7 m high, contains a sandy lens (centre of photograph) that may be aeolian in origin. The TL age obtained on the sands (≥134 ± 21 ka) (McIntosh, 2018) may be older than the actual age of deposition. The TL age supports the interpretation, first proposed by Wasson (1977) for similar exposures, that the lower 3.5 m of the deposit that has a brown matrix accumulated during the penultimate glacial period and weathered during the last interglacial period (MIS 5e) and the upper 3.5 m of the deposit that has a grey (less weathered) matrix accumulated during the last glacial cycle (MIS 5d–MIS 2).

with the stratigraphic evidence discussed by McIntosh et al. (2013) and McIntosh (2015b), supports an aeolian origin for the deposits. Particularly relevant is the observation that the sands at Mary Ann Bay are up to 24 m asl, but at Pipe Clay Lagoon, 1 km east of the bay, Colhoun (1977) found last interglacial sands near present-day sea level, and between these two sites (and in the greater Hobart region) there is no evidence of the late Pleistocene tectonic uplift postulated by Murray-Wallace and Woodroffe (2014, p. 218) to explain the present elevation of the shelly layer.

The 31–25 ka age for the sandy matrix is not incompatible with the last interglacial age obtained for the shells. The intact shells in the upper part of the aeolian deposit imply that a nearby relict shell bank was eroded during the late last glacial period (after 31–25 ka) and shells were blown up dune stoss slopes to higher altitude by strong westerlies. This interpretation supports the arguments of Petit et al. (1981) and Zhou et al. (1994) that the climate was windier during the LGM than in the preceding period. It is noteworthy that wind gusts of 100 km/h or more have been recorded in every month of the year at Hobart airport (19 km north of Mary Ann Bay; Figure 1) and a maximum wind speed of 130 km/h was recorded in October, 1988 (BOM, 2020; record for station 94008). Experiments on the wind speeds required to move the largest Mary Ann Bay shells could establish the maximum wind speeds in the late last glacial period for this exposed site.

Upper Derwent estuary (New Norfolk to Hobart)

Wasson (1977) was unable to date the fan deposits he described in the upper Derwent estuary. However, since Wasson's study three TL ages for sediments overlain or enclosed by fan gravels have been obtained. At Granton, a sandy lens, possibly of aeolian origin, in a shallow erosion channel within the fan deposits, was TL dated ≥134 ± 21 ka (McIntosh, 2018; Fig. 8). The sample did not display a lengthy TL temperature plateau (D. Price, written communication, 21 May 2014), so the TL signal may not have been completely reset before the lens accumulated. Consequently, this age may not represent a true depositional age, which may be younger. Single-grain OSL dating could resolve the age uncertainty.

The gravels below the sandy lens have a brown sandy clay matrix whereas those above have a grey matrix (Fig. 8). The age obtained and the colour difference suggest that the sandy lens marks the boundary between fan gravels that weathered during the last interglacial period but accumulated in the penultimate glacial period (MIS 6), whereas the overlying less-weathered fan gravels accumulated in the last glacial cycle (MIS 5d–2). The sandy lens may have resulted from aeolian activity during the MIS 5e/5d transition as the climate rapidly became colder and drier. The Derwent River has undoubtedly been a source of aeolian deposits at Granton: within 1 km of the Granton fan Colhoun (2002, figure 12) recorded a section of aeolian fine sand (since destroyed) which he described as loess.

At New Norfolk, sands preserved under fan gravels were TL dated >87.5 ± 7.4 and 74.1 ± 9.1 ka (McIntosh et al., 2012, fig. 10). The sands are deduced to be part of a dune derived from the Derwent River floodplain which at present is 60 m west of the outcrop.

At Blackstone Point on the east side of the Derwent estuary near Hobart, Sigleo and Colhoun (1982) described a 2 m-thick sandsheet covering about 20 ha. It consisted of four sandy layers overlying estuarine sands, silts and gravels assumed to be of last interglacial age. The lower two sand units (Units 1 and 2) contained Aboriginal artefacts, hearths, and transported remains of edible mussels so are likely to be younger than 40 ka. Radiocarbon ages of around 6.5 cal ka BP (Table 1) were obtained for charcoal and mussels in the second oldest layer (Unit 2) and these ages, and the position of the Aboriginal site near the present coastline, suggest that all the sands here are Mid- to Late Holocene.

At Bridgewater, Sigleo and Colhoun (1982) described a 2 m-thick sandsheet of similar dimensions to that at Blackstone Point, overlying alluvial gravels and dolerite. It lies immediately east (i.e., downwind) of a broad east-west reach of the Derwent River. Charcoal in an Aboriginal midden at 60 cm depth was dated 4.540 ± 0.105 ^{14}C ka BP (4.87–5.47 cal ka BP) (Table 1), but the sands below the midden (which do not contain Aboriginal artefacts) may date to the last glacial period, as the now-drowned floodplain of the Derwent River, which is very wide (1.5 km) for 2.5 km upstream (west) of the deposit, is the obvious source area.

Jordan River Dune

East of the Jordan River at Glenfield is a low dune up to 2.5 m thick in which Sigleo and Colhoun (1982) identified four

aeolian units with three palaeosols. Aboriginal hearths and artefacts were found in Unit 2 (second from the top) and the oldest radiocarbon age obtained was 2.055 ± 0.120 ^{14}C ka BP (1.78–2.33 cal ka BP).

Much older OSL ages (37.5–26.6 ka) were obtained by Paton (2010) for a deposit containing Aboriginal artefacts adjacent to and south of the Jordan River at Brighton, 2 km north of Glenfield. This deposit was described as a levee by Paton (2010) but inspection by the corresponding author of this paper revealed loose fine sands indistinguishable from near-source inland dunes found nearby (e.g., those described by Sigleo and Colhoun, 1982) or found in the Midlands, and therefore a dune interpretation (McIntosh et al., 2012) is preferred. The OSL ages obtained by Paton (2010) were disputed by Olley (2010) and the dating issue needs to be resolved by resampling and single-grain OSL analysis. If the dunesand with artefacts is confirmed as being close to 40,000 years old it is the oldest non-habitation Aboriginal site in Tasmania and approximately equal in age to the oldest habitation site known at Wareen Cave (Allen, 1996). As the 37.5 ka age was obtained close to the base of the dune it is possible that the dune started to accumulate following catchment erosion and increased bedload in the Jordan River resulting from vegetation fires lit by the Aboriginal population.

Near-source dunes and aeolian deposits of the southern forests

In the Arve and Huon valleys east of Geeveston in southern Tasmania, annual rainfall increases from about 1350 mm in the Arve valley to over 1600 mm further west at Warra on the Huon River. At present these areas support dense eucalypt forests with some trees up to 100 m high. Rainforest occurs in areas relatively protected from wildfires. Dunes in both these areas attest to a much drier climate in the past.

Southwood A dune

At the Southwood A site in the Arve valley an isolated dune occurs on a ridge at 190 m altitude and was TL dated 18.7 ± 1.2 ka and 19.1 ± 1.3 ka (McIntosh et al., 2008, 2012; Fig. 9), indicating unobstructed movement of sand from a source in the west (the Arve River floodplain) in an open or sparsely vegetated environment during the LGM, possibly during the same brief period of high winds that was responsible for the accumulation of intact shells in the upper (undated) sandy deposits at Mary Ann Bay described above. That the vegetation was sparse enough to allow dune movement implies a semi-arid climate at this location in the LGM. The soils in the area are predominantly shallow and formed in Permian and Triassic siltstones and sandstones, but at Southwood A the deposit underlying the dune is a deeply weathered fan deposit formed in part from dolerite which has weathered to reddish-brown clay (Fig. 8). This clayey soil is likely to have retained more moisture than the surrounding shallow silty and sandy soils and favoured better vegetation cover, which could have been instrumental in trapping aeolian deposits at this location.

Southwood B dune

Further north in the Arve River catchment (Fig. 10) a road section of sandy deposits 3 m deep was TL dated 60–28 ka (McIntosh et al., 2009). The section was later redated using OSL and TT-OSL techniques by Neudorf et al. (2019), who also obtained OSL and TT-OSL ages from samples collected from below road level to 5.53 m depth (samples SB4–SB7) (Table 3). The base of the section was not reached.

The source area for the Southwood B deposits is likely to have been the Willamette Creek floodplain (within 100 m of the dune) and the Arve River floodplain approximately 1.5 km to the west. Undated longitudinal quartzose dunes forming east-west ridges approximately 3 m high and up to 600 m long occur on the Arve River floodplain and on terraces of Willamette creek, immediately west of Southwood B (Fig. 10).

Well-developed organic-rich palaeosols are absent in the Southwood B stratigraphic column but several stratigraphic breaks, marked either by an underlying horizon with greater clay content, or better developed soil structure, or charcoal fragments, are interpreted to be weakly-developed palaeosols. There are no indications in the profile of an intensity of weathering resembling that in the present-day soil, or of major disconformities. The original TL age of the topmost sample (27.9 ± 2.1 ka; W4014) is older than the revised OSL and TT-OSL age (19.7 ± 2.2 ka) from the same sample (Table 3). This is probably because the TL ages have not been corrected for any surface (modern) sample residual dose (D. Price, personal communication), and they were measured using multiple aliquot techniques that determine one age value for a sample (Shepherd and Price, 1990), rather than a distribution of age values, from which a minimum age can be calculated (Galbraith et al., 1999). Therefore, the OSL and TT-OSL age estimate for W4014 (19.7 ± 2.2 ka) is considered most accurate (Neudorf et al., 2019); it is similar to the ages (18.7 ± 1.2 ka and 19.1 ± 1.3 ka) obtained for the Southwood A dune (Fig. 8).

One sample (W4013 from 0.96–1.06 m depth) gave a TL age (55.4 ± 3.0 ka) out of the expected age order, which suggested that either there has been local reworking of aeolian sediment without total resetting of the TL signal, or that near-source alluvial grains retaining a previous TL signal have been incorporated into the aeolian deposit with only partial resetting (McIntosh et al., 2009). However, when these TL ages were recalculated using dose rates measured by neutron activation analysis from the same samples (Neudorf et al., 2019), the ages of samples W4011, W4012, W4013 were equivalent within 1 sigma (see revised figures in Table 3), and the ages of underlying samples W4009 and W4010 were slightly younger (Neudorf et al., 2019). Because this apparent age reversal appears to affect all methods of equivalent dose (De) measurement (TL, OSL and TT-OSL), the reversal is likely caused by spatial variations in environmental dose rate that have not been taken into account in our dose rate

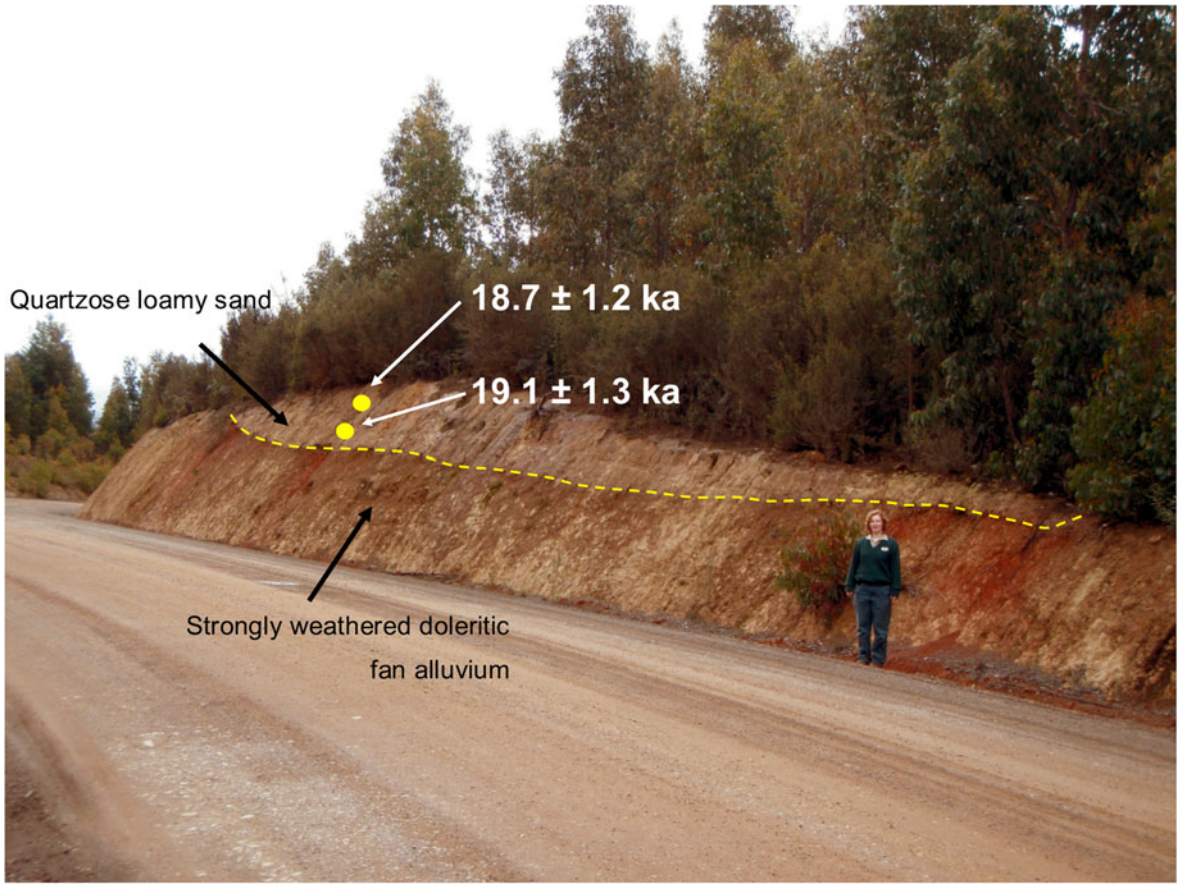

Figure 9. (colour online) The Southwood A dune, consisting of quartzose sand overlying red-weathered doleritic fan alluvium. The dune accumulated in the LGM, at ca.19 ka.

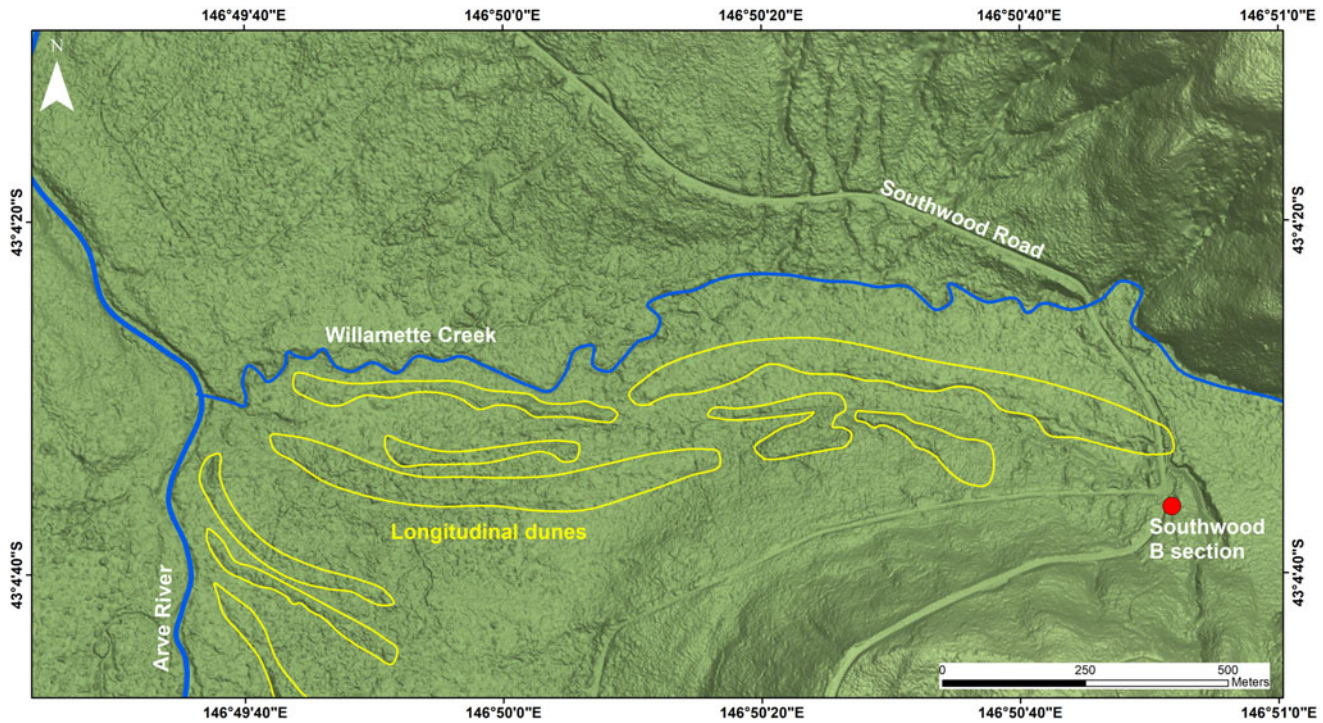

Figure 10. (colour online) Longitudinal dunes west of Southwood B.

Table 4. Interpretation of palaeolandscape processes and palaeoclimate from the Maynes Junction site.

Layer	TL ages and ^{14}C ages	Landscape and climate interpretation
Present day soil in colluvium		Soil developed in the **warm and wet** Holocene climate; colluvium accumulated during the late LGM, when vegetation cover was not complete, in a **dry climate**, probably aided by freeze-thaw processes.
White silty/fine sandy layer at ca. 0.5 m depth	W4947 (TL) **19.6 ± 1.4 ka**	Aeolian silt/fine sand accumulated in **semi-arid conditions** during the LGM (MIS 2).
Strongly developed palaeosol	Not dated	Colluvium; indicates hillslope instability after 30 ka and before 20 ka; the climate was mostly **cool and dry**. However, strong soil development occurred under a **moist and mild** climate (possibly under forest cover) for a brief period before 19.6 ka.
White silty/fine sandy layer at ca. 1 m depth	Wk26704 (AMS) 26.931 ± 0.351 ^{14}C ka BP (**30.500–31.500 cal ka BP**)	Aeolian silt/fine sand accumulated in **semi-arid** conditions during MIS 3 or late MIS 4.
Brown mottled colluvium	Not dated	Colluvium formed in a poorly-vegetated and **cool and dry** landscape with seasonal soil saturation; MIS 4?
White silty/fine sandy layer at ca. 2.5 m depth	W4968 (TL) **90.2 ± 10.2 ka**	Aeolian silt/fine sand accumulated in **semi-arid conditions** during late MIS 5c or MIS 5b.

measurements. Charcoal sampled at ca. 1.5 m depth (the same depth as TL sample W4012) was AMS dated >40 ^{14}C ka BP (uncalibrated) (Table 3), i.e., as expected from the revised TL age (49.7 ± 5.9 ka) the charcoal is beyond the range of radiocarbon dating.

Revised TL ages from samples W4009 and W4010 agree (within error) with both the OSL and TT-OSL age estimates of coeval sample SB3, providing confidence in the TL, OSL and TT-OSL dating methods. The OSL and TT-OSL chronology from samples SB4 through SB7 lower in the section increases with depth from 49 ka to 184 ka, which puts the aeolian sediments at ~5.5 m depth into MIS 6.

The Southwood B section is one of the longest known records of aeolian deposition at a non-coastal site in Australia, and demonstrates intermittent deposition of sand and silt for about 165,000 years. The overall rate of accumulation of sediment in the upper portion of the section (0.46 m to 3.35 m depth) is about 0.10 mm per year, five times higher than the rate of accumulation (about 0.02 mm per year) of underlying sediments at 3.85 m to 5.53 m depth. Assuming little or no loss of accumulated sediment by erosion, these data may indicate windier and/or drier conditions during MIS 2–4 than in earlier cold episodes, or, alternatively, greater supply of sand and silt from nearby sources (floodplains) during this period.

Warra

At Warra in the Huon River valley southwest of Hobart, a narrow strip of dunes occurs on a terrace forming the north bank of the Huon River. A dune 2.5 m deep was excavated and a sample of sand taken from 2.0 m depth gave a TL age of 40.6 ± 1.2 ka (W4553; McIntosh, 2012a). One kilometre west of this site aeolian sands at Slees Cutting were TL dated 34 ± 1.7 ka and 33.5 ± 1.8 ka (McIntosh et al., 2009). The ages obtained show that the bouldery terrace underlying the aeolian deposits at both sites is 41 ka old or older. The coincidence of the older age with the arrival of Aborigines in southern Tasmania at ca. 40 ka (Allen, 1996) may be significant: it is possible that both in the Huon River catchment, and also in the Jordan River catchment upstream of the site described by Paton (2010), a dry climate and drought-tolerant vegetation, combined with increased fire frequency following Aboriginal arrival (in order to facilitate movement and provide enhanced grazing areas for wildlife; Gammage, 2011; Fletcher et al., 2020) led to increased erosion (Macphail and Jackson, 1978; McIntosh et al., 2009; Fletcher and Thomas, 2010), which in turn increased the supply of sandy source material to river floodplains and led to dune accumulation.

Maynes Junction

At Maynes Junction at 42.776°S (Fig. 11), three prominent white or grey silty or fine sandy layers were dated by radiocarbon and TL methods (McIntosh 2012b; Table 4). These are overlain and separated by layers formed in gravelly colluvium derived from Permian siltstone, which has weathered to brown-coloured gravelly clays or silty clays, as described by Grant et al. (1995). Published information was supplemented with two new TL ages, particle-size analysis, and chemical analysis (see Supplementary Material for methods and derivation of TL ages).

An interpretation of the genesis of the Maynes Junction exposure is given in Table 4. The pale layers cannot be explained by current or past pedological processes: the soils are not poorly drained or gleyed, nor do they contain evidence (e.g., angular Permian gravels) indicating that they result from pedogenic clay eluviation from a subsoil horizon formed in gravelly colluvium which is ubiquitous on slopes around this site.

Analysis (Table 5) shows that the top and lowest pale layers contain more than 60% silt and have the lowest clay

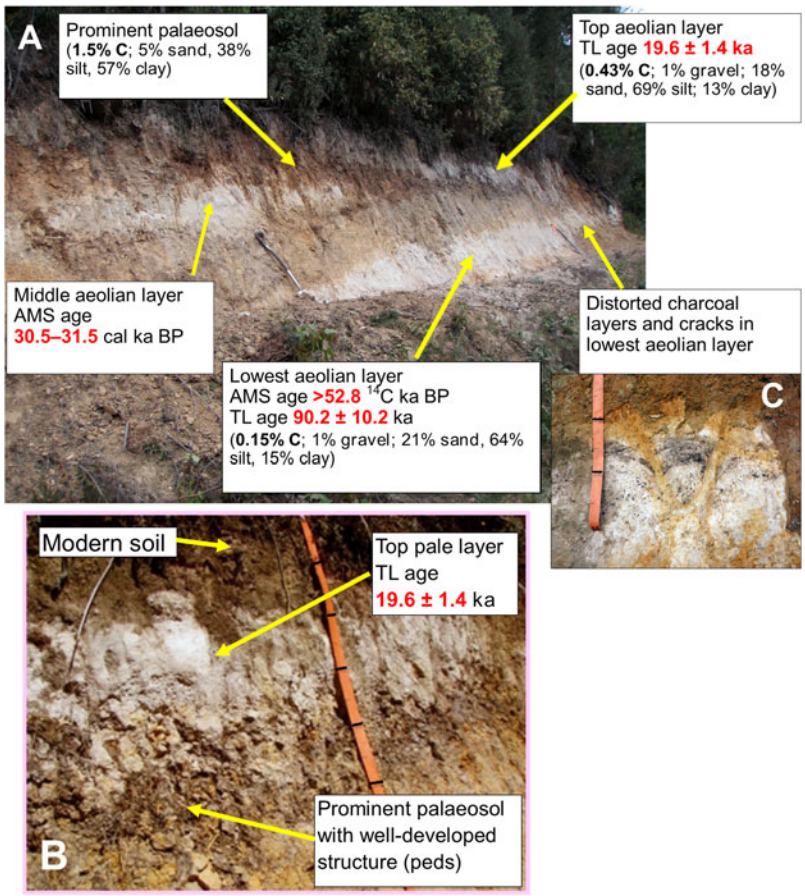

Figure 11. (A) General view of the Maynes Junction section, showing the three pale layers interpreted to be aeolian, separated by brown colluvium derived from weathered Permian siltstone; foreground spade is 1 m long. (B) Detail of the well-structured palaeosol underlying the top pale layer; tape is marked at 10 cm intervals. (C) Prominent distorted charcoal band and infilled cracks in lowest aeolian layer; tape is marked at 10 cm intervals. (For interpretation of the references to colour in this figure legend, the reader is referred to the web version of this article.)

percentage of any layers in the profile; they are also dominated by quartz, and consequently have high silica content. Permian gravels which are plentiful in the yellowish-brown clayey layers are almost absent in the pale layers; those present may have been derived from upslope. As the pale layers differ both in texture and silica content from the intervening weathered colluvium and from Permian colluvium in nearby soils they are likely to have originated from an allochthonous silica-rich source, i.e., they were probably introduced by aeolian processes. The most likely source for the pale aeolian layers is the wide (2.5 km) combined floodplain of the Tyenna River and Kallista Creek 3–5 km northwest of Maynes Junction, where boreholes up to 30 m deep have revealed intermittent (but undated) accumulations of quartzose silts and sands (figs. 4 and 5 in Walker, 2016; Mineral Resources Tasmania cores BH2 and BH3). Sediment supply to floodplains may have been enhanced during periods of snow melt on nearby mountains, for example from the glaciated Mt. Mueller (1245 m asl).

That dry conditions prevailed when the aeolian layers were deposited is illustrated by the cracks developed in the lowest aeolian layer (Figure 11C) (64% silt and 15% clay, Table 5). Such cracks (called "gammations" in New Zealand) are typical of Pallic soils developed in widespread silty loess of similar particle size distribution that accumulated during the dry and cold last glacial period on the terraces and rolling land of the eastern South Island of New Zealand lowlands in seasonally dry areas (Bruce, 1971; fig. 2 in McIntosh, 1984; Manaaki Whenua Soils Portal, 2020).

Noteworthy is the TL age of the upper aeolian deposit (19.6 ± 1.4 ka) which closely matches the two TL ages (18.7 ± 1.2 and 19.1 ± 1.3 ka) for the isolated dune at Southwood A and the OSL/TT-OSL age for the topmost layer at Southwood B (19.7 ± 2.2 ka). (These ages are within the range [24 ± 2 to 19 ± 2 ka] of siliceous aeolian sand accumulation north of Bass Strait at Cape Liptrap on the Victorian coast [Gardner et al. {2006}] and within the range [23.8 ± 1.6 to 16.8 ± 0.9 ka] of the ages of the Ainslie Dunes in northeast Tasmania.) Like the Southwood A isolated dune, Maynes Junction is distant from likely sources such as floodplains, indicating accumulation in a dry semi-arid environment with sparse vegetation cover between the site and the source area, but sufficient vegetation at the accumulation site to trap airborne or saltating sediment during the late LGM.

A palaeosol with well-developed soil structure (blocky peds) immediately underlies the topmost pale layer at Maynes

Table 5. Particle-size analysis and silica content of layers at Maynes Junction.

Layer[1]	Depth (cm)	Particle size				XRF analyses
		<2 mm fraction			>2 mm fraction	
		Clay (%)	Silt (%)	Sand (%)	Gravel (%)	SiO_2 (%)
Present-day topsoil	0–12	22	55	23	4	73
	12–30	17	59	24	1	86
Top pale layer	30–70	13	69	18	1	94
Palaeosol	70–100	57	38	5	0	58
	100–125	38	47	15	27	63
	125–160	38	46	16	11	72
Lowest pale layer	160–220	15	64	21	1	94
	220–240	23	57	19	2	89
	240–260	24	57	19	14	87
	310–400	37	54	9	15	60

[1]Note that the section analysed did not intersect the middle pale layer described in Table 4.

Junction (Fig. 11). The high clay content and well-developed soil structure of the palaeosol resembles soils formed under forest cover today, suggesting that it was formed in a moist climate, possibly under forest vegetation, and was buried when dry conditions and aeolian deposition recommenced at around 20 ka. A period of moister conditions immediately prior to a final episode of dry cold stadial conditions after 22.5 ka is also recorded in the Dunlin Dune record, where a podzol formed after 21.0 ± 1.5 ka, before being buried by renewed dune-building which began before 15.9 ka. If the prominent palaeosol at Maynes Junction can be assigned to the same post-21.5 ka wet period as that recorded at Dunlin Dune, then the moist period at Maynes Junction must have occurred between about 21.0 ± 1.5 ka and 19.6 ± 1.4 ka, i.e. it lasted about 1000–2000 years.

Evidence from other sites (Fig. 12) supports a moist interval between approximately 21 and 20 ka: (1) the Antarctic (EPICA C) dust record is highly variable in the 21–19.6 ka period, with dust levels varying almost tenfold (149 µg/kg to 1470 µg/kg) in this time interval (Delmonte et al., 2004), implying climatic instability over sub-millennial periods of time; (2) at Lake Surprise (39.06°S) in Victoria, Australia, Falster et al. (2018, figure 4) recorded low aeolian Si inputs and moister conditions for plants between 21 and 20 ka; (3) speleothem records from Mt. Arthur (41.22°S) in New Zealand indicate that forest productivity increased rapidly for a short period between 21 and 20 ka between two $\delta^{18}O$ excursions (MD3/5 and MD3/4) that correlate with glacial advances (table 2 and fig. 7 in Hellstrom et al., 1998); (4) at Galway Tarn in south Westland, New Zealand (43.41°S), Vandergoes et al. (2013) also record a brief interstadial period (Gt5) immediately preceding the final LGM stadial, but it occurs earlier (ca. 22.6–21.8 cal ka BP); as does (5) a peak of eucalypt cover at 18.240 ± 0.100 ^{14}C ka BP (22.37–21.85 cal ka BP) recorded at Hazards Lagoon (42.17°S) on the Tasmanian east coast (Mackenzie and Moss, 2014).

A likely influence on rainfall and vegetation cover at Maynes Junction is oscillation of the subantarctic front: its retreat southwards would be accompanied by milder and wetter conditions while its advance northwards over Tasmania would increase aridity on account of the cooler waters around southeast Australia (Falster et al., 2018, p. 119). Such changes can cause surface sea temperature changes of ca. 6°C within 100 years (Barrows et al., 2007).

The middle pale layer at Maynes Junction (Table 4, Figure 11) (AMS dated 26.931 ± 0.351 ^{14}C ka BP [30.50–31.50 cal ka BP]) probably formed during the same dry episode that gave rise to the deep silty and sandy aeolian gully infill at Cradoc Hill (TL dated 31.8 ± 1.4 to 25.3 ± 1.3 ka) (McIntosh et al., 2004); the partly aeolian gully infill at Maynes Hill (AMS dated 24.475 ± 0.288 ^{14}C ka BP [29.47–28.17 cal ka BP]); similar infill at Sharps Gully (TL dated 30.1 ± 0.3 to 23.5 ± 1.7 ka and AMS dated 25.175 ± 0.261 ^{14}C ka BP [28.64–29.93 cal ka BP]) (McIntosh et al., 2008, 2012); the younger deposits at Llanherne (TL dated ca. 26 ka); and the extensive aeolian deposits at Mary Ann Bay (TL and OSL dated in the range 31–25 ka). These six sites indicate that from about 30 ka to 23 ka (spanning the late MIS 3 and early MIS 2) conditions favouring deflation from source areas and accumulation at vegetated or protected downwind sites prevailed in southern Tasmania. Significantly, there was also a phase of deposition at ca. 27 ka on southern Prime Seal Island. As discussed for particular sites, increased droughtiness, increased sediment supply (from fluvial sources) and/or land exposure from receding sea levels, and increased windiness may all have played a part in inducing wind erosion and concurrent deposition of aeolian sediment at this time.

Aeolian deposits dating to MIS 4 are not present in the Maynes Junction record. The lowest pale layer at Maynes Junction with the TL age of 90.2 ± 10.2 ka has not been described as a distinct layer elsewhere, but it may correspond with the deposit dated 84.1 ± 5.5 ka at Southwood B (Table 3). It indicates a dry period favouring aeolian activity in MIS 5c.

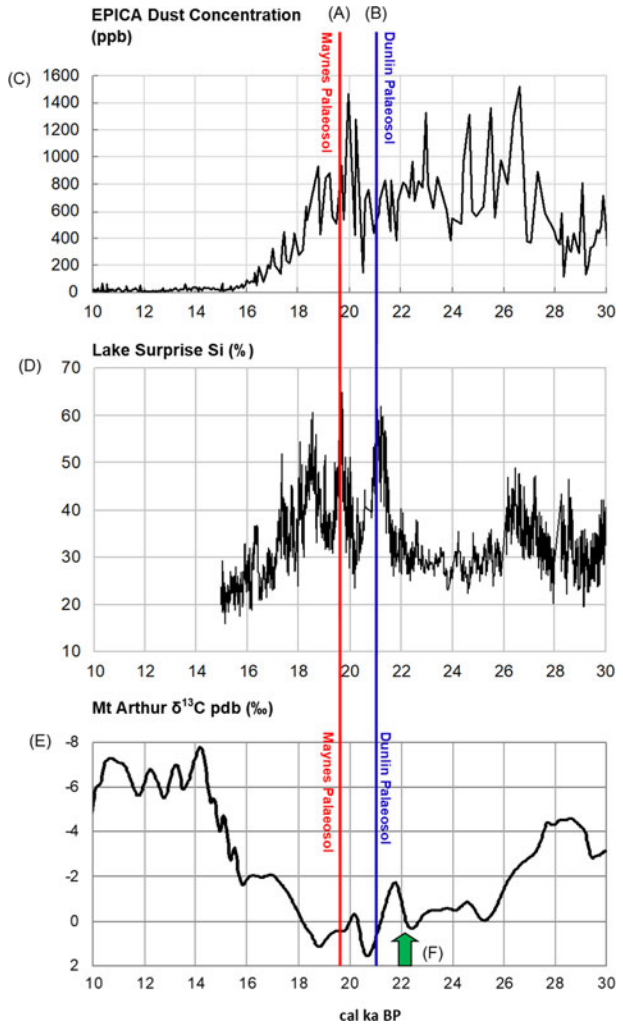

Figure 12. Suggested correlations of Maynes Junction palaeosols and Dunlin Dune palaeosol with other climatic indicators: (A) the red line indicates the TL age (19.6 ± 1.4 ka) of the upper aeolian deposit at Maynes Junction; this is the *minimum* age of the palaeosol below; (B) the blue line indicates the TL age (21.0 ± 1.5 ka) of the sediment in which a palaeosol has formed in the Dunlin Dune; this is the *maximum* age of the palaeosol; (C) the EPICA dust record from Dome C, Antarctica (Delmonte et al., 2004); (D) percentage of Si in the Lake Surprise core, Victoria, Australia (Falster et al., 2018); (E) $\delta^{13}C$ in a speleothem from Mt. Arthur, South Island, New Zealand (Hellstrom et al., 1998); (F) the green arrow indicates the median radiocarbon age (22.1 cal ka BP) of eucalypt increase in the Hazards Lagoon core, Tasmania (Mackenzie and Moss, 2014) and the median radiocarbon age (22.2 cal ka BP) of the small trees and shrubs peak in the Galway Tarn record from South Island, New Zealand (Vandergoes et al., 2013). (For interpretation of the references to colour in this figure legend, the reader is referred to the web version of this article.)

CONCLUSIONS

Tasmania has extensive aeolian deposits. Remnants of longitudinal desert dunes that formed at the margins of the now-flooded Bassian Plain are found in northern mainland Tasmania. Last glacial ages (24–16 ka) have been obtained, mostly from upper layers of these dunes, but they probably started forming much earlier. Sands dated 56 ka on Prime Seal Island in the Furneaux Group, and 60 ka at Rocky Point on King Island, are also likely to be remnants of Bassian Plain inland dunes formed when the sea level was much lower, but their original form has been largely destroyed by later erosion and dune building. The location and age of these deposits suggest a widespread and broadly concurrent onset of semi-arid or arid conditions conducive to aeolian transport of sediment across northern Tasmania and the Bassian Plain commencing late in MIS 4 and continuing to MIS 2.

Other extensive aeolian terrains on King Island, and those on Flinders Island, lungtalanana (Clarke Island) and Hunter Island provide further evidence for the scale and timing of aeolian influences on the Bassian Plain. The aeolian deposits on these islands are mostly poorly described and undated, but many deposits are assumed to have a last glacial age, based on ages obtained for similar deposits on Prime Seal Island and in northeast Tasmania. In contrast, the field evidence indicates that inland dunes located at the eastern margin of the Yellow Rock River basin on King Island are interglacial deposits formed during high sea levels, probably in MIS 9.

Sandsheets, dunes and deflation basins with associated lunettes on their downwind (eastern) sides are common in eastern Tasmania and the subhumid Tasmanian Midlands but none have been dated, except for charcoal relating to late Aboriginal occupation. Under the present subhumid climate these deposits are stable; they indicate a period of semi-arid climate when tree cover was minimal and chenopod grasslands with intervening bare ground dominated (Macphail and Jackson, 1978), allowing greater supply of sediment from eroding streams and bare floodplains, particularly where the deflation basins were fed by runoff and erosion from adjacent uplands.

Dunes are extensive in inland Tasmania and in coastal areas of the south and west. The most complete record is at the Southwood B site in the Arve River catchment, where deposition over a period of 165 ka is recorded. The presence of both isolated and longitudinal inland dunes in areas of the Arve and Huon valleys that now receive >1350 mm of rain per annum attest to the greater extent of dry conditions in the last glacial period. Many coastal dunes are Holocene in age, but remnants of dunes dating to 60–56 ka on the Tasmanian west coast including King Island indicate widespread aeolian activity on the much wider coastal plains that existed in the last glacial period. Other dunes and aeolian deposits (sandsheets and gully infills) date to 40 ka and later, with several sites having aeolian deposits dating to 31–23 ka. The most extensive and thickest deposits in this period are those dated 31–25 ka at Mary Ann Bay on the South Arm Peninsula (Slee et al., 2012; Shin, 2013). These deposits are part of a widespread and probably continuous cold-climate sandsheet that formed east of the lower Derwent River estuary (their assumed source) and included aeolian deposits at other sites nearby (Donaldson, 2010). Low-lying parts of this area have since been eroded and inundated by rising sea level, leaving only higher aeolian remnants.

The Maynes Junction section in southern Tasmania has recorded repeated episodes of aeolian deposition and intervening periods of hillslope instability. The aeolian deposits are deduced to be derived from deflation of quartzose silt and fine sand from upwind floodplains. Extensive deposition on these floodplains is likely to have resulted from snow melt in the mountains west of Maynes Junction, e.g., from Mt. Mueller (1245 m asl). The stratigraphy at Maynes Junction allows climatic changes to be interpreted from 90 ka to the Holocene: three periods of aeolian deposition around 90 ka, 30 ka, and 19.7 ka are recorded, separated by two milder periods. In one of these periods, pronounced soil development occurred, probably under forest vegetation, indicating that within the LGM, at approximately 21–20 ka, there was a short-lived relatively mild and wet period likely to have been caused by a southerly shift of the subantarctic front, favouring higher rainfall in the west and southwest (and probably concurrent expansion of forests) due to the more frequent passage of depressions over Tasmania. This brief mild interval was followed by resumed dry conditions in the coldest period of the LGM which induced a final phase of aeolian activity at around 19 ka. The deduced climatic oscillations at Maynes Junction match those recorded at Lake Surprise in Victoria (Falster et al., 2018) and in New Zealand (Hellstrom et al., 1998), but the mild interval in New Zealand dated by Vandergoes et al. (2013) was earlier than that recorded at Maynes Junction.

The observations summarised in this review raise several issues regarding the climatic conditions required to induce formation of dunes and other aeolian deposits. The formation of coastal dunes is undoubtedly largely supply-dependent, and some inland dunes, such as those at Warra (close to the Huon River) and the longitudinal dunes west of the Southwood B deposit (downwind of the Arve River floodplain) may also be largely explained by pulses of sediment supply resulting from sparse vegetation cover on floodplains and on uplands where seasonal snow melt may have been a major factor inducing flooding and erosion on lowlands. Early Holocene transverse dunes dated 10.1 ± 1.2 ka near Strahan are also likely to have accumulated as a result of increased sediment supply to lowland floodplains during the final stages of glacial ice melt on the West Coast Range. The evidence from other sites, such as the Southwood A dune perched relatively high in the landscape over a patch of water-retentive doleritic soils in a sandstone landscape with shallow soils, suggest that sparse cover of vegetation in the surrounding area, probably induced by a semi-arid climate, has facilitated dune movement over several kilometres. In contrast the many lunettes (all undated) downwind (east) of ephemeral lakes in the Tasmanian Midlands have accumulated close to sources (lagoons), which may indicate the presence of stabilising vegetation at lake margins. However, associated with these lunettes are more subtle dune forms and sandsheets, and these landforms, along with the only pollen record for an ephemeral lake in the area (Macphail and Jackson, 1978), are evidence for a semi-arid climate with an intermittent land cover of low vegetation, probably in late last glacial period.

Whether wind speeds were higher during the last glacial period is uncertain. Petit et al. (1981) and Zhou et al. (1994) argued for higher wind speeds to explain aerosol deposition in East Antarctica and Victoria, Australia, respectively, and Fletcher and Thomas (2010) suggested that an expanded high pressure system over the Australian mainland coupled with greater extent of sea ice to the south of Tasmania could have resulted in stronger westerly winds (and higher rainfall) than at present on the west coast of Tasmania and stronger and drier foehn winds in the east. Bowden (1983) calculated that the wind speeds required to explain particle size distribution in the Ainslie dunes in northeast Tasmania must have been about 30% stronger than at present. Hesse (1994) initially accepted that wind speeds were probably higher during glacial periods, but in later papers (Hesse and McTainsh, 1999, 2003) proposed that mid-latitude westerlies in the Australian region were no stronger during the last glacial period than in the Holocene, and argued that dust supply rather than wind speed was the prime driver of aeolian sedimentation in mainland Australia and the Tasman Sea. However Bowden's conclusions (Bowden, 1983) have not been refuted, and his study, and the inclusion of shells in the aeolian deposits of the exposed site at Mary Ann Bay, suggest that in Tasmania higher wind speeds may well have contributed to the extensive aeolian deposits found in the state, although patchy low vegetation (partly induced by drought and partly by low CO_2 concentrations [Bragg et al., 2012]), greater deflation from unvegetated river floodplains fed by snow melt, and burning of vegetation by the Aboriginal population are also likely to have had an influence.

ACKNOWLEDGMENTS

This study was partly supported by research funds provided by the board of the Forest Practices Authority, Tasmania. O.B. Lian acknowledges support from a Natural Sciences and Engineering Research Council (NSERC) of Canada Discovery Grant and an NSERC Research Tools and Equipment Grant. C.M. Neudorf was supported by a Hakai Postdoctoral Fellowship while at the University of the Fraser Valley, BC, Canada. D.P. Price of the University of Wollongong undertook the TL analyses. The cooperation of Sustainable Timbers Tasmania (formerly Forestry Tasmania) in allowing research and sampling within state forests is gratefully acknowledged. We thank J. Shulmeister and D. Booth and two anonymous reviewers for their constructive suggestions for improving the manuscript.

SUPPLEMENTARY MATERIAL

The supplementary material for this article can be found at https://doi.org/10.1017/qua.2020.83.

REFERENCES

Allen, J. (Ed.), 1996. Report of the Southern Forests Archaeological Project. Vol. 1, Site Descriptions, Stratigraphies and Chronologies. Archaeology Publications, School of Archaeology, La Trobe University.

Barrows, T.T., Juggins, S., De Dekker, P., Calvo, E., Pelejero, C., 2007. Long-term sea-surface temperatures and climate change in the Australian-New Zealand region. *Paleooceanography* 22, 2215.

Baynes, F.J., 1990. A Preliminary Survey of the Coastal Geomorphology of the World Heritage Area, South West Tasmania. Unpublished Report for the Department of Parks, Wildlife and Heritage, Tasmania.

Blom, W.M., 1988. Late Quaternary sediments and sea levels in Bass basin, southeastern Australia–a preliminary report. *Search* 19, 94–96.

Bowden, A.R., 1983. Relict terrestrial dunes: legacies of a former climate in coastal northeastern Tasmania. *Zeitschrift für Geomophologie* Supplement 45, 153–174.

Bowler, J.M., 1998. Willandra lakes revisited: environmental framework for human occupation. *Archaeology in Oceania* 33, 120–155.

Bowler, J.M., Price, D.M., 1998. Luminescence dates and stratigrahic analyses at Lake Mungo: review and new perspectives. *Archaeology in Oceania* 33, 156–168.

Bowler, J.M., Wasson, R.J., 1984. Glacial age environments of arid Australia. *Transactions, Institute of British Geographers* 56, 77–110.

Bradbury, J., 1994. Aeolian Landforms in the Lake Ada - Lake Augusta area: A Preliminary Investigation and Management Strategy. Draft Report of National Parks and Wildlife Service. Department of Primary Industries and Water, Tasmania.

Bradbury, J., 2014. A revised geological map of lungtalanana (Clarke Island) and brief explanatory notes. In: Natural and Cultural Heritage Division. lungtalanana (Clarke Island), Natural Values Survey 2014. Hamish Saunders Memorial Trust, New Zealand and Natural and Cultural Heritage Division, DPIPWE, Hobart. Nature Conservation Report Series 15/2, pp. 36–61.

Bragg, F.J., Prentice, I.C., Harrison, S.P., Eglinton, G., Foster, P.N., Rommerskirchen, F., Rullkőtter, J., 2012. Stable isotope and modelling evidence that CO_2 drives vegetation changes in the tropics. *Biogeosciences Discussions* 9, 156699–15722.

Bronk Ramsey, C., 2009. Bayesian analysis of radiocarbon dates. *Radiocarbon* 51, 337–360.

Bruce, J.G., 1971. Loessial deposits in southern South Island, with a definition of Stewarts Claim formation. *New Zealand Journal of Geology and Geophysics* 16, 533–548.

Bureau of Meterology, 2020. Climate statistics for Australian locations. http://www.bom.gov.au/climate/averages/tables/cw_094008_All.shtml

Calver, C.R., 2007. Some notes on the geology of King Island. Tasmania Geological Survey Record 2007/02, Department of Infrastructure, Mineral Resources, Tasmania.

Colhoun, E.A., 1977. A sequence of late Quaternary deposits at Pipe Clay Lagoon, southeastern Tasmania. *Papers and Proceedings of the Royal Society of Tasmania* 111, 1–12.

Colhoun, E.A., 1985. Glaciations of the West Coast Range, Tasmania. *Quaternary Research* 24, 39–59.

Colhoun, E.A., 2002. Periglacial landforms and deposits of Tasmania. *South African Journal of Science* 98, 55–63.

Colhoun, E.A., Turner, E., van der Geer, G., 1982. Late Pleistocene molluscan faunas from four sites in Tasmania. *Papers and Proceedings of the Royal Society of Tasmania* 166, 91–96.

Comfort, M., Eberhard, R., 2011. The Tasmanian geoconservation database: a tool for promoting the conservation and sustainable management of geodiversity. *Proceedings of the Linnean Society of New South Wales* 132, 27–36.

Compton, J.S., 2011. Pleistocene sea-level fluctuations and human evolution on the southern coastal plain of South Africa. *Quaternary Science Reviews* 30, 506–527.

Cosgrove, R., 1985. New evidence for early Holocene Aboriginal occupation in northeast Tasmania. *Australian Archaeology* 21, 19–36.

Cullen, P., Dell, M., 2013. Geomorphological evolution of the Prion Beach and New River Lagoon beach barrier system. Nature Conservation Report Series 2013/03. Department of Primary Industries, Parks, Water and Environment, Tasmania.

Delmonte, B, Basile-Doelsch, I., Petit, J.-R., Maggi, V., Revel-Rolland, M., Michard, A., Jagoutz, E., Grousset, F., 2004. Comparing the Epica and Vostok dust records during the last 220,000 years: stratigraphical correlation and provenance in glacial periods. *Earth Science Reviews* 66, 63–87.

Dixon, G., 1996. A reconnaissance inventory of sites of geoconservation significance on Tasmanian islands. Report for Parks and Wildlife Service, Tasmania and Australian Heritage Commission, Canberra.

Dixon, G., 1997. A preliminary survey of the distribution and conservation significance of inland aeolian features in the Midlands, Northeast and Southeast Tasmania. Parks and Wildlife Service, Tasmania.

Donaldson, P., 2010. *Facies architecture and radar stratigraphy of the Seven Mile Spit complex, Tasmania*. Unpublished Honours thesis, School of Earth Sciences, University of Tasmania.

Doyle, R.B., 1993. Soils of the South Esk Sheet Tasmania (southern half). Soil Survey Series of Tasmania No. 1. Department of Primary Industries and Fisheries, Tasmania.

Duller, G.A.T., Augustinus, P., 1997. Luminescence studies of dunes from north-eastern Tasmania. *Quaternary Science Reviews* (*Quaternary Geochronology*) 16, 357–365.

Duller, G.A.T., Augustinus, P., 2006. Reassessment of the record of linear dune activity in Tasmania using optical dating. *Quaternary Science Reviews* 25, 2608–2618.

Eberhard, R., 2009. Geodiversity. In: Harris, S., Driessen, M., Bell, P. (Eds). Prime Seal Island Scientific Expedition 2008. Hamish Saunders Memorial Trust, New Zealand and Biodiversity Conservation Branch, DPIPWE, Hobart, Nature Conservation Report Series 09/3, pp. 10–25.

Eberhard, R., 2017. Aspects of geodiversity on Hunter Island: four Quaternary age geosites. In: Natural and Cultural Heritage Division, South Hunter and Stack Island Natural and Cultural Values Survey. Hamish Saunders Memorial Trust, New Zealand and the Natural and Cultural Heritage Division, DPIPWE, Hobart. Nature Conservation Report 17/4, pp. 68–90.

Eberhard, R., Sharples, C., Bowden, N., Comfort, M., 2015. Monitoring the Erosion Status of Oceanic Beaches in the Tasmania Wilderness World Heritage Area: Establishment Report. Nature Conservation Report Series 15/3. Natural & Cultural Heritage Division, Department of Primary Industries, Parks, Water & Environment, Hobart.

Falster, G., Tyler, J., Grant, K., Tibby, J., Turney, C., Lőhr, S., Jacobsen, G., Kershaw, A.P., 2018. Millennial-scale variability in south-east Australian hydroclimate between 30,000 and 10,000 years ago. *Quaternary Science Reviews* 192, 106–122.

Fletcher, M-S., Hall, T., Alexandra, A.N., 2020. The loss of an indigenous constructed landscape following British invasion of Australia: an insight into the deep human imprint on the Australian landscape. *Ambio*. https://doi.org/10.1007/s13280-020-01339-3.

Fletcher, M-S., Thomas, I., 2010. The origin and temporal development of an ancient cultural landscape. *Journal of Biogeography* 37, 2183–2196.

Galbraith, R.F., Roberts, R.G., Laslett, G.M., Yoshida, H., Olley, J.M., 1999. Optical dating of single and multiple grains of quartz from Jinmium rock shelter, northern Australia: Part I, experimental design and statistical models. *Archaeometry* 41, 339–364.

Gammage, B., 2011. The Biggest Estate on Earth: How Aborigines made Australia. Allen & Unwin, Sydney.

Gardner, T.W., Webb, J., Davis, A.G., Cassel, E.J., Pezzia, C., Merrits, D.J., Smith, B., 2006. Late Pleistocene landscape response to climate change: eolian and alluvial fan deposition, Cape Liptrap, southeastern Australia. *Quaternary Science Reviews* 25, 1552–1569.

Gillespie, R., Camens, A.B., Worthy, T.H., Rawlence, N.J., Reid, C., Bertuch, F., Levchenko, V., Cooper, A., 2012. Man and megafauna in Tasmania: closing the gap. *Quaternary Science Reviews* 37, 38–47.

Grant, J.C., Laffan, M.D., Hill, R.B., Neilsen, W.A., 1995. Forest Soils of Tasmania. Forestry Tasmania, Hobart.

Hellstrom, J., McCulloch, M., Stone, J., 1998. A detailed 31,000 year record of climate and vegetation change, from isotope geochemistry of two New Zealand speleothems. *Quaternary Research* 50, 167–178.

Hesse, P.P., 1994. The record of continental dust from Australia in Tasman Sea sediments. *Quaternary Science Reviews* 13, 257–272.

Hesse, P.P., 2016. How do longitudinal dunes respond to climate forcing? Insights from 25 years of luminescence dating of the Australian desert dunefields. *Quaternary International* 410, 11–29.

Hesse, P.P., Humphreys, G.S., Smith, B.L., Campbell, J., Peterson, E.K., 2003. Age of loess deposits in the central tablelands of New South Wales. *Australian Journal of Soil Research* 41, 1115–1131.

Hesse, P.P., McTainsh, G.H., 1999. Last glacial maximum to early Holocene wind strength in the mid-latitudes of the southern hemisphere from aeolian dust in the Tasman Sea. *Quaternary Research* 52, 343–349.

Hesse, P.P., McTainsh, G.H., 2003. Australian dust deposits: modern processes and the Quaternary record. *Quaternary Science Reviews* 22, 2007–2035.

Jennings, J.N., 1957. Coastal dune lakes as exemplified from King Island, Tasmania. *Geographical Journal* 123, 59–70.

Jennings, J.N., 1959. The coastal geomorphology of King Island, Bass Strait in relation to changes in the relative level of land and sea. *Records of the Queen Victoria Museum* 11, 1–39.

Johnson, C., 2006. Australia's Mammal Extinctions: A 50 000 year History. Cambridge University Press. Melbourne.

Kershaw, R.C., Sutherland, F.L., 1972. Quaternary geomorphology on Flinders Island. *Records of the Queen Victoria Museum* 43, 28 pp.

Lambeck, K., Chappell, J., 2001. Sea level change through the last glacial cycle. *Science* 292, 679–685.

Lewis, S.E., Sloss, C.R., Murray-Wallace, C.V., Woodroffe, C.D., Smithers, S.G., 2013. Post-glacial sea-level changes around the Australian margin: a review. *Quaternary Science Reviews* 74, 115–138.

Lisiecki, L.E., Raymo, M.E., 2005. A Pliocene-Pleistocene stack of 57 globally distributed benthic δ18O records. *Paleoceanography* 20, dx.doi.org/10.1029/2004PA001071.

Lourandos, H., 1970. *Coast and Hinterland: The Archaeological Sites of Eastern Tasmania*. Thesis, Department of Prehistory and Anthropology, Australian National University, Canberra.

Mackenzie, L., Moss, P., 2014. A late Quaternary record of vegetation and climate change from Hazards Lagoon, eastern Tasmania. *Quaternary International* 432, 58–65.

Macphail, M.K., Jackson, W.D., 1978. The late Pleistocene and Holocene history of the Midlands of Tasmania. *Proceedings of the Royal Society of Victoria* 90, 287–300.

Manaaki Whenua Soils Portal, 2020. https://soils.landcareresearch.co.nz/describing-soils/nzsc/soil-order/pallic-soils (accessed 20 March 2020).

Matthews, W.L., 1975. Geological atlas 1:50,000 series, Lake River. Tasmania Department of Mines, Hobart.

Matthews, W.L., 1983. Geology and groundwater resources of the Longford Tertiary basin. *Geological Survey Bulletin* 59. Tasmania Department of Mines.

Mazengarb, C., Stevenson, M.D., 2016. Pleistocene coastal terraces in northern Tasmania revisited; what do they tell us about landscape evolution and uplift rates? Presented paper, AESC 2016 – Australian Earth Sciences Convention; Uncover Earth's Past to Discover Our Future, Adelaide Convention Centre. Geological Society of Australia.

McClenaghan, M.P. (Compiler), 2006. Digital Geological Atlas 1:25000 series, Sheet 5447, Waterhouse. Mineral Resources Tasmania, Rosny.

McIntosh, P.D., 1984. Genesis and classification of a sequence of soils formed from aeolian parent materials in East Otago, New Zealand. *Australian Journal of Soil Research* 22, 219–242.

McIntosh, P.D., 2012a. Soil characterisation at the Warra Flux Tower supersite. Version 2, with supplementary data. Forest Practices Authority Contract Report, prepared for Forestry Tasmania, 16 pp.

McIntosh, P.D., 2012b. Dated geoconservation sites in the forest estate in Tasmania, 2004–2012. Forest Practices Authority Technical Report 2. Forest Practices Authority, Hobart.

McIntosh, P.D., 2015a. Soils and Land Capability in the Kempton–Melton Mowbray Road Corridor. Contract report for State Growth, April 2015. Forest Practices Authority, Hobart, 19 pp.

McIntosh, P.D., 2015b. Comments on the paper 'Stratigraphy and geochronology of Quaternary marine terraces of Tasmania, Southeastern Australia: implications on neotectonism by Jaeryul Shin, Geosciences Journal 17, p. 429–443'. *Geosciences Journal* 19, 575–578.

McIntosh, P.D., 2018. Dating Wasson's Derwent Valley fans. *Quaternary Australasia* 35, 9.

McIntosh, P.D., Eberhard, R., Slee, A., Moss, P., Price, D.M., Donaldson, P., Doyle, R., Martins, J., 2012. Late Quaternary extra-glacial cold-climate deposits in low and mid-altitude Tasmania and their climatic implications. *Geomorphology* 179, 21–39.

McIntosh, P.D., Kiernan, K., Price, D.M., 2004. An aeolian sediment pulse at c. 28 kyr BP in southern Tasmania. *Journal of the Royal Society of New Zealand* 34, 369–379.

McIntosh, P.D., Price, D.M., Eberhard, R., Slee, A., 2008. Late Quaternary erosion chronology in lowland and mid-altitude Tasmania. Forest Practices Authority, *Scientific Report* 5.

McIntosh, P.D., Price, D.M., Eberhard, R., Slee, A.J., 2009. Late Quaternary erosion events in lowland and mid-altitude Tasmania in relation to climate change and first human arrival. *Quaternary Science Reviews* 28, 850–872.

McIntosh P.D., Price, D.M., Grove, S., Slee, A.J., 2013. 'Reply to Murray-Wallace et al. (2013): comments on a paper by Slee et al. (2012). A reassessment of last interglacial deposits at Mary Ann Bay, Tasmania'. *Quaternary Australasia* 30, 4–8.

Murray-Wallace, C.V., Goede, A., 1991. Aminostratigraphy and electron spin resonance dating of late Quaternary sea level change and coastal neotectonics in Tasmania, Australia. *Zeitschift für Geomorphologie* 35, 129–149.

Murray-Wallace, C.V., Goede, A., 1995. Aminostratigraphy and electron spin resonance dating of Quaternary coastal neotectonism in Tasmania and the Bass Strait islands. *Australian Journal of Earth Sciences* 42, 51–67.

Murray-Wallace, C.V., Woodroffe, C.D., 2014. Quaternary Sea-Level Changes: A Global Perspective. Cambridge University Press. Cambridge, England.

Murray, A.S., Wintle, A.G., 2000. Luminescence dating of quartz using an improved single aliquot regenerative dose protocol. *Radiation Measurements* 32, 57–73.

Nanson, G.C., Chen, X.Y., Price, D.M., 1995. Aeolian and fluvial evidence of changing climate and wind patterns during the past 100 ka in the western Simpson Desert, Australia. *Palaeogeography, Palaeoclimatology, Palaeoecology* 113, 87–102.

Neudorf, C.M., Lian, O.B., McIntosh, P.D., Gingerich, T.B., Augustinus, P.C., 2019. Investigation into the OSL and TT-OSL signal characteristics of ancient (>100 ka) Tasmanian aeolian quartz and its utility as a geochronometer for understanding long-term climate-driven landscape change. *Quaternary Geochronology* 53, 101005.

Olley, J., 2010. Peer review of the TASI 10757 Jordan River, Brighton, Tasmania: luminescence chronology (Cupper, May 2010). Unpublished Griffith University Report to Department of Primary Industries, Parks, Water and Environment, Hobart, Tasmania.

Osok, R., Doyle, R., 2004. Soil development on dolerite and its implications for landscape history in southeastern Tasmania. *Geoderma* 121, 169–186.

Paton, R., 2010. Draft Final Archaeology Report on the Test Excavations of the Jordan River Levee Site, southern Tasmania. Robert Paton Archaeological Studies Pty Ltd, Tasmania.

Petit, J.-R., Briat, M., Royer, A., 1981. Ice age aerosol content from East Antarctic ice core samples and past wind strength. *Nature* 293, 391–394.

Pinkard, G.J., 1980. Land Systems of Tasmania, Region 4. Tasmanian Department of Agriculture, Hobart.

Reffet, E., Courrech du Pont, S., Hersen, P., Douady, S., 2010. Formation and stability of transverse and longitudinal sand dunes. *Geology* 38, 491–494..

Reimer, P.J., Bard, E., Bayliss, A., Beck, J.W., Blackwell, P.G., Ramsey, C.B., Buck, C.E., *et al*., 2013. IntCal13 and Marine13 radiocarbon age calibration curves 0–50,000 years cal BP. *Radiocarbon* 55, 1869–1887.

Rule, S., Brook, B.W., Haberle, S.G., Turney, C.S.M., Kershaw, A.P., Johnson, C.N., 2012. The aftermath of megafaunal extinction: ecosystem transformation in Pleistocene Australia. *Science* 335, 1483–1486.

Sharples, C., 1996. A Reconnaissance of Landforms and Geological Sites of Geoconservation Significance in the Murchison Forest District. Report to Forestry Tasmania. (2 vols.)

Sharples, C., 1997. Geoconservation Survey of Bridport - Waterhouse Telstra Cable Route. Report for Telstra Corporation Ltd, Hobart.

Sharples, C., Walford, H., Watson, C., Ellison, J.C., Hua, Q., Bowden, N., Bowman, D., 2020. Ocean Beach, Tasmania: a swell-dominated shoreline reaches climate-induced recessional tipping point? *Marine Geology* 419, 106081.

Shepherd, M.J., Price, D.M., 1990. Thermoluminescence dating of late Quaternary dunesand, Manawatu/Horowhenua area, New Zealand, a comparison with ^{14}C age determinations. *New Zealand Journal of Geology and Geophysics* 33, 535–539.

Shin, J., 2013. Stratigraphy and geochronology of Quaternary marine terraces of Tasmania, southeastern Australia: implications on neotectonism. *Geosciences Journal* 17, 429–443.

Sigleo, W.R., Colhoun, W.A., 1982. Terrestrial dunes, man and the late Quaternary environment in southern Tasmania. *Palaeogeography, Palaeoclimatology, Palaeoecology* 39, 87–121.

Slee, A.J., McIntosh, P.D., Price, D.M., Grove, S., 2012. A reassessment of last interglacial deposits at Mary Ann Bay, Tasmania. *Quaternary Australasia* 29, 4–11.

Sutherland, F.L., Kershaw, R.C., 1971. The Cainozoic geology of Flinders Island, Bass Strait. *Papers and Proceedings of the Royal Society of Tasmania* 105, 151–176.

Turney, C.S.M., Flannery, T.F., Roberts, R.G., Reid, C., Fifield, L.K., Higham, T.F.G., Jacobs, Z., *et al*., 2008. Late-surviving megafauna in Tasmania, Australia, implicate human involvement in their extinction. *Proceedings of the National Academy of Sciences* 105, 12150–12153.

Twidale, C.R., 1957. A reconnaissance of the Corinna-Pieman Heads area – geomorphology. *Papers and Proceedings of the Royal Society of Tasmania* 91, 9–17.

Vandergoes, M.J., Newnham, R.M., Denton, G. H., Blaauw, M., Barrell, D.J.A., 2013. The anatomy of last glacial maximum climate variations in south Westland, New Zealand, derived from pollen records. *Quaternary Science Reviews* 74, 215–229.

Walker, B.J.R., 2016. *Late Pleistocene climatic oscillations inferred by soil stratigraphic analysis of southern Tasmanian Quaternary sediments*. Honours Thesis, University of Tasmania.

Wasson, R.J., 1977. Catchment processes and the evolution of alluvial fans in the Lower Derwent valley, Tasmania. *Zeitschrift für Geomorphologie* 21, 147–168.

Wasson, R.J., Hyde, R., 1983. Factors determining desert dune type. *Nature* 304, 337–339.

Zhou, L., Williams, M.A.J., Petersen, J.A., 1994. Late Quaternary aeolianites, palaeosols and depositional environments on the Nepean peninsula, Victoria, Australia. *Quaternary Science Reviews* 13, 225–239.

SUPPLEMENTARY MATERIAL

LUMINESCENCE DATING

Aeolian landforms in Tasmania, and in Australia in general, have been dated mainly by luminescence methods. Indeed, the advent of luminescence dating has revolutionised the understanding of aeolian environments (e.g., Singhvi and Porat, 2008; Duller, 2016) and of late Quaternary history in general (Roberts and Lian, 2015).

Luminescence dating is based on the premise that natural minerals contain impurities and structural defects that can act as traps for free electrons. At ambient temperatures some of these traps can hold electrons for only a few hours or less, but there are others that can hold them for millions of years or more, and these are referred to as thermally stable or deep traps. All traps can be emptied by exposure to sufficient heat (~400°C), but only some traps can be emptied by exposure to light. Free electrons are produced when minerals absorbs ambient radiation. If a sediment sample is buried in a sedimentary landform, for example, electron traps in the mineral grains will fill at a rate proportional to the production of free electrons, the environmental dose rate. If the sediment sample is uncovered and exposed to a few seconds of direct sunlight, light-sensitive electron traps will be emptied. If the sample is exposed to sufficient heat, both light-sensitive and light-insensitive traps will be emptied. In the laboratory, experiments are designed that allow for an estimate to be made of the dose of laboratory radiation that will produce the same intensity of luminescence as the dose absorbed by the sample in the environment since burial; this is referred to as the equivalent dose. A sample's luminescence age is simply its equivalent dose divided by its environmental dose rate. The various luminescence

dating methods that have been developed since the 1960s mainly involve variations in the technique used to estimate equivalent dose, and in the methods by which the most light-sensitive thermally stable traps are selected. The evolution of luminescence dating techniques, and their design and applicability has been reviewed in detail by Lian and Roberts (2006) and Wintle (2008) and in these reviews illustrative examples are also given; a concise account is given below, with an emphasis on quartz as it has been the preferred chronometer for dating aeolian landforms in Australia.

Thermoluminescence dating

Luminescence dating has its roots in thermoluminescence (TL) dating of fired material such as pottery (Aitken et al. (1964, 1968); and see review by Roberts (1997)). The first detailed accounts of reliable methods for TL dating sunlight-exposed sediments were reported by Wintle and Huntley (1979a, b, 1980, 1982). The most widely used TL dating methods are relatively similar in that to estimate equivalent dose they rely on the measurement of many multi-grain aliquots of prepared sediment. The simplest methods involve leaving some of the aliquots as is (the ‘naturals’, N), while the remainder are given various increasing doses of laboratory radiation producing an N+dose set of aliquots. All of the aliquots are heated one at a time in an inert atmosphere from room temperature to about 600°C while the TL is recorded; each aliquot produces a plot of TL intensity as a function of temperature, which is often called a glow curve. Glow curves consist of several overlapping peaks that represent trap populations with various sensitivities to light and different thermal stabilities; the peaks that appear at higher temperatures are those that are thermally stable over time periods of interest.

In the simplest case an equivalent dose value is estimated by plotting the TL measured at a particular temperature as a function of laboratory dose, which produces a dose-response curve (or 'growth curve'). The TL recorded from the natural aliquot(s) is interpolated onto the dose-response curve to find the equivalent dose (Wintle and Huntley, 1982, fig. 1b). If the heating causes sensitivity change in the mineral being analysed, then a different approach is needed. This involves plotting the N and N+dose aliquots together, fitting a curve to all the data, and extrapolating it to where it intersects the dose axis (Wintle and Huntley 1982, fig. 1c). An expansion of this method accounts for the presence of a residual TL signal (from incomplete, or partial bleaching prior to burial). This method involves exposing some of the natural and dosed aliquots to a short duration of light to empty the most light-sensitive traps, producing a separate N+dose+bleach set of aliquots. The growth curves from both sets of aliquots are plotted on the same graph and extrapolated to where they intersect above the dose axis, and the equivalent dose is read at that point. This is the 'partial bleach' technique (Wintle and Huntley, 1982, fig. 9). In some cases the partial bleach technique is simplified by replacing the N+dose+bleach set of aliquots by a single N+bleach point and a line is extended from it to where it intersects the N+dose curve. In other cases, where it is suspected that the sample received extended sunlight exposure prior to burial, the N+dose+bleach set (or N+bleach aliquot) is given a longer sunlight bleach to empty all light-sensitive traps, and this is referred to as the 'total bleach' method (Wintle and Huntley, 1979 a; Singhvi et al., 1982). Another approach is to give a set of aliquots prolonged exposure to light, to entirely remove the light-sensitive TL signal, and then give them various doses to construct an N+bleach+dose (regenerative) set. This regenerative set of data is shifted onto the

N+dose set, and the magnitude of the shift is taken as the equivalent dose value; this technique is referred to as the ‘Australian Slide’ (AS) method due to its initial application to date a sequence of ancient coastal dunes in South Australia (Prescott et al. 1993). This method is preferred when the extrapolation of dose response curves required for the partial bleach method is large, which is common for old samples. The Australian Slide method also has the advantage of detecting the presence of any sensitivity change in the mineral (incurred by dosing, bleaching, and heating the sample in the laboratory) by comparing quantitatively the shapes of the two growth curves.

For TL dating techniques, growth curves are constructed at various read temperatures, and these produce a set of equivalent dose values that are plotted as a function of temperature. For a sample that has received sufficient sunlight exposure prior to burial, and for which growth curve data are fitted with the appropriate function (curve), the equivalent dose values should plot as a plateau, and, for quartz, if this is the case, values between 325 and 400 °C (e.g., Huntley and Prescott, 2001) are typically averaged and used together with the sample’s environmental dose rate to estimate a TL age.

Optically stimulated luminescence dating

A new luminescence dating technique was developed by Huntley et al. (1985) in which luminescence is produced by stimulation with light of a specific wavelength, or wavelength range, instead of by heat. This technique is called optical dating, and it is also commonly referred to as optically-stimulated luminescence (OSL) dating. It has advantages over TL dating in that the most light-sensitive electron traps can be measured directly (the OSL signal bleaches much more rapidly than the TL signal), and the experimental setup is simpler which leads to better precision. The first OSL

dating techniques were developed directly from those used for TL dating and therefore also required that many aliquots be made to construct dose response curves. Because aliquots cannot be made to be identical, they are normalised using the OSL measured over a short duration before any doses of laboratory radiation are administered. Since laboratory irradiation populates both thermally stable and thermally unstable traps, the aliquots are heated together before the OSL is measured to empty electrons from thermally unstable traps which would not have remained filled in the environment over geological timescales. This ‘preheating’ sometimes causes the unwanted transfer of electrons from light-insensitive traps to the traps of interest for dating, but it can be accounted for by including an N+dose+bleach set of aliquots (Huntley et al., 1993). Aliquots are measured one at a time and the OSL is recorded as a function of time, typically for 50 or 100 s. The result is a luminescence decay curve (shine-down curve) for each aliquot which is the sum of several individual curves (signal components), each representing a specific trap or trap population. For quartz, some of these signal components are useful for dating, while others are not; not all quartz samples have the same signal components, and the prominence of these components vary from sample to sample, and even between aliquots or single grains of the same sample. Dose response curves are constructed over intervals of measurement time and this approach can be used to crudely select the signal components of interest (there are more complex methods that can be used to more thoroughly and objectively separate signal components). Equivalent dose is found by extrapolation of the N+dose and N+dose+bleach data to where they intersect above the dose axis. In some cases the N+dose+bleach curve is omitted, if thermal transfer is found to be negligible, or it is replaced by a single N+bleach point as is done in the total bleach method used in TL

dating. The AS method, already described for TL dating, is also applicable to OSL dating.

The single-aliquot regenerative-dose (SAR) technique

Shortly after the development of the first multiple aliquot OSL dating methods, protocols were introduced that allowed an equivalent dose value to be determined from a single aliquot of prepared sediment, which could consist many grains or just a single grain (Stokes, 1994; Murray and Roberts, 1997). This allows for much small sample sizes to be measured, and samples that consist of populations of grains with various environmental bleaching histories, or different luminescence signal characteristics, can potentially be scrutinised; it also eliminates the need for normalisation. This lead to the development of statistical techniques that can be used to estimate representative equivalent dose values (and ages) from those produced from many aliquots (e.g., Galbraith et al., 1999; Roberts et al., 2000).

The first single aliquot techniques consisted of a simple single-aliquot additive-dose (SAAD) protocol, and a ‘single-aliquot regeneration and added-dose’ (SARA) protocol (Mejdahl and Bøtter-Jensen, 1994). But because these protocols required that each aliquot be dosed, heated, and measured several times, the sensitivity of the aliquot changed with each cycle (e.g., Armitage et al., 2000) and this had to be corrected for. This correction was usually done by monitoring sensitivity changes in a second aliquot of the same sample. These methods were therefore not strictly single-aliquot protocols, but they later became so by instead monitoring changes to the sensitivity in the 110°C TL peak (for quartz). This approach was later improved further by alternatively monitoring sensitivity changes in the OSL measured after a ‘test dose’, which is administered immediately after the OSL is measured from the natural and each regenerative dose. This protocol includes internal checks for

thermal transfer (recuperation) and for the efficacy of the chosen test dose to correct for sensitivity change, and it also called for a subsequent experiment to test the utility of the protocol to recover a known dose of laboratory radiation, similar in magnitude to what it had absorbed in the environment (the dose recovery test). It has become the standard single-aliquot regenerative-dose (SAR) protocol used today for dating both quartz (Murray and Wintle, 2000, 2003; Wintle and Murray, 2006) and feldspar. Subsequent development has included use of different OSL signals, such as the thermally-transferred OSL signal from quartz, which is discussed below in the context of this paper, to extend the upper age limit of the method.

Age evaluation and sources of uncertainty

It is important to recognise that all luminescence dating techniques are inherently experimental. This is because the luminescence characteristics of quartz (and feldspar) vary from site to site, and even within a single site. Preliminary experiments are therefore usually conducted to ascertain the character of the OSL (or TL) signal in order to identify and isolate the most easily bleached thermally-stable component(s) and to identify the most efficient preheat temperature(s). The factors that lead to uncertainty in the determination of a sample's environmental dose rate are site dependent, and are influenced by uncertainty about a sample's water content and its burial depth over time, by the degree of knowledge of local variations in the concentrations of relevant radioisotopes in the sediment matrix (on both the macro and micro scales), and how these may have changed over time, and by assumptions made about the degree of equilibrium in their decay chains. There are also uncertainties associated with the radioisotope content within the grains, but this is relatively minor when dating quartz. And of course the fundamental conditions that the mineral grains sampled were exposed to sufficient sunlight prior to burial, and

that they have not been mixed with older or younger grain populations after burial, has to be satisfied (or at least accounted for later) and this is not always the case even for aeolian sediments (e.g., Lian and Huntley, 1999; Cohen et al., 2010).

The best check to see if a luminescence dating protocol is able to effectively estimate burial age at a particular site is to compare ages with those derived using reliable independent method at the same stratigraphic position. This was proposed as an acceptance criterion in one of the seminal papers on luminescence dating of sediments (Wintle and Huntley, 1982). In practice, however, this is often difficult to do when working with aeolian landforms, especially dunes, as the applicability of other dating methods to the aeolian environment is rare; however, good consistency has been found in many cases, for example, see Rhodes (2011, fig. 10). Moreover, not all practitioners publish experimental procedures with the same level of detail, and this commonly makes comparison between studies challenging, and differences in ages, even within a single study, difficult to assess. And even in cases where detailed experimental work has been performed, and has been well presented, discrepancies between ages found using different luminescence dating methods can be difficult to understand (e.g., Mueller et al., 2018). It is therefore not possible to conclude that a luminescence dating protocol(s) that has been demonstrated to be successful at one site will also be useful at another site; all that can be said is that it is likely to be successful there as well, sometimes after some modification. These sentiments have been exemplified by Hesse (2016) who provides an analysis of nearly 700 OSL and TL ages, found using various laboratory protocols, using both multiple and single aliquot techniques, associated with Australian continental aeolian dunes (coastal dunes and lunettes were excluded in his review), including those in Tasmania. He did find, however, that the published data sets of age values for this

region contained very few internal inconsistencies, such as age reversals (Hesse, 2016).

Luminescence dating methods relevant to this study

The geochronology of most sites in Tasmania discussed in this paper come mainly from TL ages derived using the method of Shepherd and Price (1990). Some sites include OSL ages determined using the SAR method (Wintle and Murray, 2000), and one site, Southwood B dune, has been dated using thermally-transferred (TT) OSL signals and the SAR method, which has been shown to be successful in dating sediments that are beyond the upper age limit of more traditional OSL methods.

The TL method of Shepherd and Price (1990)

The TL method of Shepherd and Price (1990), which essentially is that described by Readhead (1988), was developed from the early methods described above. It is a combined multiple-aliquot additive and regenerative dose procedure. The TL growth curve in this instance is derived from aliquots that have had the bleachable fractions of their TL signals removed by exposure to an ultraviolet lamp. They are then given, in groups, successively increasing (regenerative) doses of radiation prior to TL measurement. Aliquot-to-aliquot variations in TL intensity is normalised using an “irradiation/second glow” procedure, and TL sensitivity differences between the natural aliquots, and the aliquots that had been bleached in the laboratory, are checked by overlaying the first growth curve (above) with a growth curve generated from natural (unbleached) aliquots that are subsequently given a series of radiation (additive) doses, much like the sensitivity check that is inherent to the AS method. As mentioned earlier, TL ages derived using multiple aliquot techniques require many aliquots of prepared sample to generate a single age. Therefore, TL dating

techniques cannot mitigate the adverse effects of poorly bleached grains that may lead to age being overestimated. Thus TL dating is most applicable to well-bleached deposits (loess, and dunes and sandsheets constructed of distally derived material will normally fit this category) and in these instances they have been shown in many cases to yield ages consistent with those found using SAR OSL. In Tasmania, for example, TL ages for dunes at Mary Ann Bay (Slee et al., 2012) determined using the protocol of Shepherd and Price (1990) are consistent with ages found using OSL and what appears to be a SAR method (Shin 2013) (Supplementary Material, Table S1), but unfortunately Shin (2013) provides no experimental detail so a thorough assessment cannot be made.

Supplementary Material, Table S1. Comparison of TL and OSL ages obtained from Mary Ann Bay sandsheets. See the main text for details.

Depth (cm)	Laboratory I.D.	Method	Age (ka)[1]	Reference
200	MA02	OSL	31.0 ± 3.0	Shin (2013)
290-300	W4475	TL	30.7 ± 1.0	Slee et al. (2012)
600	MA05	OSL	25.0 ± 3.0	Shin (2013)
670-680	W4476	TL	30.3 ± 3.7	Slee et al. (2012)

[1]Errors are ± 1σ

Multiple-aliquot OSL and TL dating and single aliquot OSL dating

Duller and Augustinus (1997) applied three luminescence dating methods to quartz from the Ainslie dunes. The first two procedures consisted of OSL and TL multiple-aliquot methods applied to the same aliquots: the OSL signal was measured first, followed by the TL signal. A single-aliquot OSL procedure was also attempted. The

single-aliquot ages were comparable to those found using the multiple-aliquot OSL procedure, and also to three of the five TL ages.

OSL and TT-OSL dating using SAR

In light of the development of SAR protocols in the late 1990s (Wintle and Murray, 2000), Duller and Augustinus (2006) re-dated their samples from Ainslie dunes using this method. As mentioned earlier, an important difference between the SAR protocol and the earlier methods used by Duller and Augustinus (1997) is the SAR protocol's ability to correct for sensitivity change and its inclusion of internal quality control checks. The ages Duller and Augustinus (2006) determined using SAR are significantly different from those found using the older multiple-aliquot methods (Duller and Augustinus, 1997), are considered to be more accurate, and they are also consistent with palaeoclimate interpretations for the region. They also cast doubt on the general applicability of the older methods.

OSL dating using SAR methods with multi-grain aliquots or single grains has become much more routine in Tasmania (see Neudorf et al., 2019, table S1), and an extension of that method that uses the TT-OSL signal, which has been shown to extend the upper age limit of quartz OSL dating (Wang et al., 2006), has been applied at Southwood B dunes (Neudorf et al., 2019). As mentioned earlier, traditional OSL dating protocols involve heating ('preheating') the sample to a predefined temperature to empty electrons in thermally unstable traps, and then stimulating the sample with blue light (for quartz) to measure the luminescence resulting from thermally-stable traps. TT-OSL dating, on the other hand, involves heating, then stimulating the sample as one would when using a traditional OSL dating protocol, but then heating the sample again to high temperature (e.g., 290°C)

before measuring the luminescence signal a second time. This signal results from the second high-temperature preheat, which thermally transfers charge from less-optically sensitive traps, to optically sensitive traps that are sampled during stimulation (the TT-OSL). For a given quartz sample, growth curves generated by TT-OSL signals continue to increase with added dose when OSL growth curves tend to flatten out (or ‘saturate’), allowing the measurement of equivalent doses from older samples.

At Southwood B, a sequence of TT-OSL SAR ages were found to be consistent with those found previously using the TL dating method of Shepherd and Price (1990), but only after the dosimetry used to derive some of the TL ages was recalculated based on new radioisotope measurements (Neudorf et al., 2019); see also Table 3 and Figure 2 in the main article. Although the apparent consistency between the TL and TT-OSL SAR ages is encouraging, it should be considered with some caution as the TT-OSL SAR dating technique is still relatively novel. Moreover, as the TT-OSL signal bleaches more slowly than the OSL signal it usually requires correction for insufficient bleaching using the signal measured from a modern sample collected from a similar depositional environment.

NEW TL AGES INCORPORATED INTO THIS REVIEW

At Rocky Point (39.5985°S 144.0040°E) on the north-east coast of King Island (Figure 2) the age of beach-backing ‘New Dunes’ (Jennings, 1957) exposed within a sandblow within an otherwise vegetated coastal dune complex was investigated. Five units were distinguished by their texture and colour (Figure 2) and units 3 and 5 were sampled for TL dating using rigid opaque PVC tubes 75 mm diameter and 120

mm long. At Maynes Junction (Figure 10) the top and lowest pale layers were sampled for TL analysis by carving a 100 mm^3 block of sediment.

TL dating (Supplementary Material, Table S2) was performed using the methods described by Shepherd and Price (1990) and Nanson et al. (1991). Samples were analysed using the 90–125 μm quartz grain size fraction separated from the centre of bulk field samples. A summary of methods employed, including examples of TL glow curves, the TL versus temperature plateaus, and a representative growth curve was presented by McIntosh et al. (2009).

Supplementary Material, Table S2. Previously unpublished TL ages for Rocky Point and Maynes Junction aeolian sediments, and data used to derive the TL ages.

	Rocky Point samples			**Maynes Junction sample**	
Sample Lab No.	**W5021**	**W5022**	**W5023**	**W4947**	**W4968**
Field ID	**Unit 3 (upper)**	**Unit 3 (lower)**	**Unit 5**	**Top pale layer**	**Lowest pale layer**
TL Plateau region (°C)	300–400	275–500	275–500	275–500	275–500
Analysis temp. (°C)	375	375	375	375	375
Equivalent dose (Gy)	4.5 ± 0.5	5.0 ± 0.5	52.2 ± 3.4	35.5 ± 2.5	176 ± 20
K content (by XRF) (%)	0.168 ± 0.005	0.191 ± 0.005	0.249 ± 0.005	0.355 ± 0.005	0.520 ± 0.005
Moisture content by weight (%)	3.9 ± 3	5.0 ± 3	14.0 ± 3	11.7 ± 3	10.1 ± 3
Specific activity (U+Th) (Bq/kg)	10.0 ± 0.3	19.1 ± 0.6	27.5 ± 0.9	75.1 ± 2.0	71.1 ± 1.7
Cosmic ray contribution (assumed) (μGy/yr)	180 ± 25	180 ± 25	180 ± 25	150 ± 25	150 ± 25
Total environmental dose rate (μGy/yr)	543 ± 25	737 ± 26	872 ± 24	1813 ± 34	1951 ± 32
TL age (ka)	**8.32 ± 1.00**[1]	**6.75 ± 0.65**	**59.9 ± 4.3**	**19.6 ± 1.4**	**90.2 ± 10.2**

[1]This sample exhibited a short temperature plateau suggestive of incomplete re-setting of the TL signal.

Note: Measured and calculated values are listed here as reported by the laboratory. Since some of the measured values are reported with a precision of two significant figures, the calculated TL ages should be considered with the same precision.

PARTICLE SIZE ANALYSIS

At Maynes Junction, previously radiocarbon dated by McIntosh et al. (2012) a section on the right-hand side of the exposure (Figure 10), including the top pale layer and lowest pale layer was described. Component layers distinguished and sampled on the basis of their texture and colour (National Committee on Soil and Terrain 2009). Air-dried bulk samples were pre-treated as recommended by Cresswell et al. (2002). Samples rich in organic matter from 0-12 cm, 12-30 cm, and 70-100 cm depth were treated with H_2O_2 under gentle heating and disaggregated by addition of 25 ml of 0.05M sodium hexametaphosphate solution followed by 1 min of sonification and overnight end-over-end shaking. Dispersed samples from all sampled layers were separated into fine and coarse fractions using a 63 µm sieve. Sediment and gravel captured on the 63 µm sieve was designated the coarse fraction, and was retained for particle size analysis by dry sieving. The fine fractions were suspended in 1 L sedimentation tubes and particle size analysis was conducted by the pipette method (Cresswell et al. 2002). A 20 ml blank sample was taken from 25 ml sodium hexametaphosphate in a 1 L sedimentation tube so that a correction for the mass of the dispersant could be applied. The samples were then oven dried overnight at 105˚C and weighed. Coarse fractions (>63 µm) were thoroughly air dried and mechanically shaken through an Endecott standard sieve stack at half phi (ϕ) intervals for 10 min. Sediment weights obtained by pipette analysis were expressed as a percentage of the total weight of the < 2 mm sample. The percentage of gravel (>2 mm) in the total sample was also calculated.

X-RAY FLUORESCENCE ANALYSIS

Sub-samples of 14–16 g of <2 mm soil from the Maynes Junction soil horizons listed in Table 5 were oven dried and ground to fine powder in a tungsten carbide pneumonic mill. A melted fusion disk was prepared to homogenise the sample and ensure complete oxidation. XRF analysis was performed at the School of Earth Sciences, University of Tasmania using a ScMo 3kW side window X-ray tube and a Philips PW1480 x-ray spectrometer, following the methods of Robinson (2003). Whole rock sample powders were fused with 12‑22 flux (a pre-fused mixture consisting of 12 parts $Li_2B_4O_7$ and 22 parts $LiBO_2$) using a sample: flux ratio of 1:9 at 1100^{o}C. Corrections for mass absorption were calculated using Philips X40 software with De Jongh's calibration model and Philips' alpha coefficients.

REFERENCES

Aitken, M.J., Tite, M.S., and Reid, J., 1964. Thermoluminescent dating of ancient ceramics. Nature 202, 1032–1033.

Aitken, M.J., Zimmerman, D.W. and Fleming, S.J., 1968. Thermoluminescent dating of ancient pottery. Nature 219, 442–444.

Armitage, S.J., Duller, G.A.T., and Wintle, A.G. 2000. Quartz from South Africa: sensitivity changes as a result of thermal pretreatment. Radiation Measurements 32, 571–577.

Cohen, T.J., Nanson, G.C., Larsen, J.R., Jones, B.G., Price, D.M., Coleman, M. and Pietsch, T.J., 2010. Late Quaternary aeolian and fluvial interactions on the

Cooper Creek fan and the association between linear and source-bordering dunes, Strzelecki Desert, Australia. Quaternary Science Reviews 29, 455-471.

Cresswell, H.P., McKenzie, N.J. and Coughlan, K.J., 2002. Soil physical measurement and interpretation for land evaluation. CSIRO Publishing, Collingwood, Victoria.

Duller, G.A.T., 2016. Challenges involved in obtaining luminescence ages for long records of aridity: Examples from the Arabian Peninsula. Quaternary International 410, 69–74.

Duller, G.A.T. and Augustinus, P., 1997. Luminescence studies of dunes from north-eastern Tasmania. Quaternary Science Reviews (Quaternary Geochronology) 16, 357–365.

Duller, G.A.T. and Augustinus, P., 2006. Reassessment of the record of linear dune activity in Tasmania using optical dating. Quaternary Science Reviews 25, 2608–2618.

Galbraith, R.F., Roberts, R.G., Laslett, G.M., Yoshida, H., and Olley, J.M., 1999. Optical dating of single and multiple grains of quartz from Jinmium rock shelter, northern Australia. Part I: experimental design and statistical models. Archaeometry 41, 339–364.

Hesse, P.P., 2016. How do longitudinal dunes respond to climate forcing? Insights from 25 years of luminescence dating of the Australian desert dunefields. Quaternary International 410, 11–29.

Huntley, D.J., Godfrey-Smith, D.I., and Thewalt, M.L.W., 1985. Optical dating of sediments. Nature 313: 105-107.

Huntley, D.J., Hutton, J.T., and Prescott, J.R., 1993. Optical dating using inclusions within quartz grains. Geology 21, 1087–1090.

Huntley, D.J., and Prescott, J.R., 2001. Improved methodology and new thermoluminescence ages for the dune sequence in south-east South Australia. Quaternary Science Reviews 20, 687–699.

Jennings, J.N., 1957. Coastal dune lakes as exemplified from King Island, Tasmania. Geographical Journal 123, 59–70.

Lian, O.B., and Huntley, D.J., 1999. Optical dating of post-glacial aeolian deposits from the south-central interior of British Columbia, Canada. Quaternary Science Reviews 18, 1453–1466.

Lian, O.B. and Roberts, R.G., 2006. Dating the Quaternary: progress in luminescence dating of sediments. Quaternary Science Reviews 25, 2449–2468.

McIntosh, P.D., Price, D.M., Eberhard, R. and Slee, A.J., 2009. Late Quaternary erosion events in lowland and mid-altitude Tasmania in relation to climate change and first human arrival. Quaternary Science Reviews 28, 850–872.

McIntosh, P.D., Eberhard, R., Slee, A., Moss, P., Price, D.M., Donaldson, P., Doyle, R., and Martins, J., 2012. Late Quaternary extra-glacial cold-climate deposits in low and mid-altitude Tasmania and their climatic implications. Geomorphology 179, 21–39.

Mejdahl, V., and Bøtter-Jensen, L., 1994. Luminescence dating of archaeological materials using a new technique based on single aliquot measurements. Quaternary Science Reviews 13, 551–554.

Mueller, D., Jacobs, Z., Cohen, T.J., Price, D.M., Reinfelds, I.V., and Shulmeister, J., 2018. Revisiting an arid LGM using fluvial archives: a luminescence chronology for palaeochannels of the Murrumbidgee River, south-eastern Australia. Journal of Quaternary Science, 33: 777– 793.

Murray, A.S., and Roberts, R.G., 1997. Determining the burial time of single grains of quartz using optically stimulated luminescence. Earth and Planetary Science Letters 152, 163–180.

Murray, A.S., and Wintle, A.G., 2000. Luminescence dating of quartz using an improved single-aliquot regenerative-dose protocol. Radiation Measurements 32, 57-73.

Murray, A.S., and Wintle, A.G., 2003. The single aliquot regenerative dose protocol: potential for improvements in reliability. Radiation Measurements 37, 377–381.

Nanson, G.C., Price, D.M., Short, S.A., Young, R.W. and Jones, B.G., 1991. Comparative uranium–thorium and thermoluminescence chronologies for weathered alluvial sequences in the seasonally dry tropics of Northern Queensland, Australia. Quaternary Research 35, 347–366.

National Committee on Soil and Terrain, 2009. Australian Soil and Land Survey Field Handbook. 3rd Edition. CSIRO, Collingwood.

Neudorf, C.M., Lian, O.B., McIntosh, P.D., Gingerich, T.B., Augustinus, P.C., 2019. Investigation into the OSL and TT-OSL signal characteristics of ancient (>100 ka) Tasmanian aeolian quartz and its utility as a geochronometer for understanding long-term climate-driven landscape change. Quaternary Geochronology 53, doi.org/10.1016/j.quageo.2019.101005.

Prescott, J.R., Huntley, D.J., and Hutton, J.T., 1993. Estimation of equivalent dose in thermoluminescence dating the Australian slide method. Ancient TL 11, 1-5.

Readhead, M.L., 1988. Thermoluminescence dating study of quartz in aeolian sediments from southeastern Australia. Quaternary Science Reviews 7, 257–264.

Rhodes, E.J., 2011. Optically stimulated luminescence dating of sediments over the past 200,000 years. Annual Review of Earth and Planetary Sciences 39, 461-488.

Roberts, R.G., 1997. Luminescence dating in archaeology: from origins to optical. Radiation Measurements 27, 819–892.

Roberts, R.G., Galbraith, R.F., Yoshida, H., Laslett, G.M., Olley, J.M., 2000. Distinguishing does populations in sediment mixtures: a test of single-grain optical dating procedures using mixtures of laboratory dosed quartz. Radiation Measurements 32, 459–465.

Roberts, R.G., and Lian, O.B., 2015. Illuminating the past. Nature 520, 438–439.

Robinson, P., 2003. XRF analysis of flux-fused discs. 5th International Conference on the Analysis of Geological and Environmental Materials (presented paper). Geological Survey of Finland, Rovaniemi, Finland.

Shepherd, M.J. and Price, D.M., 1990. Thermoluminescence dating of Late Quaternary dunesand, Manawata/Horowhenua area, New Zealand, a comparison with ^{14}C age determinations. New Zealand Journal of Geology and Geophysics 33, 535–539.

Shin, J., 2013. Stratigraphy and geochronology of Quaternary marine terraces of Tasmania, southeastern Australia: implications on neotectonism. Geosciences Journal 17, 429–443.

Singhvi, A.K., Sharma, Y.P. and Agrawal, D.P., 1982. Thermoluminescence dating of sand dunes in Rajasthan, India. Nature 295, 313–315.

Singhvi, A.K., and Porat, N., 2008. Impact of luminescence dating on geomorphological and palaeoclimate research in drylands. Boreas 37, 536-558.

Stokes, S., 1994. The timing of OSL sensitivity changes in a natural quartz. Radiation Measurements 23, 601–605.

Slee, A.J., McIntosh, P.D., Price, D.M. and Grove, S., 2012. A reassessment of last Interglacial deposits at Mary Ann Bay, Tasmania. Quaternary Australasia 29 (2), 4–11.

Wang, X.L., Wintle, A.G., and Lu, Y.C., 2006. Thermally transferred luminescence in fine grained quartz from Chinese loess: basic observations. Radiation Measurements 41, 649–658.

Wintle, A.G., 2008. Luminescence dating: where it has been and where it is going. Boreas 37, 471–482.

Wintle, A.G., Huntley, D.J. 1979a. Thermoluminescence dating of a deep-sea sediment core. Nature 289, 479–480.

Wintle, A.G., and Huntley, D.J., 1979b. Thermoluminescence dating of sediments. PACT 3, 374–380.

Wintle, A.G., and Huntley, D.J., 1980. Thermoluminescence dating of ocean sediments. Canadian Journal of Earth Sciences 17, 348–360.

Wintle, A.G., and Huntley, D.J., 1982. Thermoluminescence dating of sediments. Quaternary Science Reviews 1, 31–53.

Wintle, A. G., and Murray, A. S., 2006. A review of quartz optically stimulated luminescence characteristics and their relevance in single-aliquot regeneration dating protocols. Radiation Measurements 41, 369–391.